EurJIC European Journal of Inorganic Chemistry

ChemPubSoc Europe

FULL PAPER

DOI:10.1002/ejic.201402087

Synthesis and Structures of Fluorinated (β-Diketiminato)-rhodium Complexes: Si–H Activation of Silanes at a Carbonyl Complex

Gregor Meier,[a] Viktoria Steck,[a] Beatrice Braun,[a] Anna Eißler,[a] Roy Herrmann,[a] Mike Ahrens,[a] Reik Laubenstein,[a] and Thomas Braun*[a]

Keywords: N ligands / Fluorinated ligands / Silicon / Silanes / Rhodium

The (β-ketiminato)rhodium complex [Rh{κ²-(*N*,*O*)-(*t*Bu)(*O*)-CCHC(*t*Bu)*N*(C_6F_5)}(cod)] (**1**) [cod = (1*Z*,5*Z*)-1,5-cyclooctadiene] and (β-diketiminato)rhodium complexes [Rh{κ²-(*N*,*N*)-(Ar)*N*C(Me)CHC(Me)*N*(Ar)}(L^1)(L^2)] [**2**: Ar = C_6F_5, (L^1)-(L^2) = cod; **3**: Ar = C_6F_5, L^1 = L^2 = C_2H_4; **4**: Ar = C_6F_5, L^1 = L^2 = CN*t*Bu; **5**: Ar = 2,6-MeC_6H_3, L^1 = L^2 = CN*t*Bu; **6a**: Ar = C_6F_5, L^1 = L^2 = CO; **7a**: Ar = C_6F_5, L^1 = CO, L^2 = NCMe; **8a**: Ar = C_6F_5, L^1 = CO, L^2 = PEt_3; **9a**: Ar = C_6F_5, L^1 = CO, L^2 = NH_3] were synthesized. Treatment of [Rh{κ²-(*N*,*N*)-(C_6F_5)-*N*C(Me)CHC(Me)*N*(C_6F_5)}(CO)(NCMe)] (**7a**) with tertiary silanes $HSiR_3$ gave the (β-diketiminato)(hydrido)(silyl)rhodium complexes [Rh{κ²-(*N*,*N*)-(C_6F_5)*N*C(Me)CHC(Me)*N*(C_6F_5)}-(H)(SiR_3)(CO)] (**10a**: R = Me; **11**: R = Et; **12**: R = *i*Pr; **13**: R = Ph; **14**: R = OMe; **15**: R = OEt). When using an excess amount of $HSiMe_3$ the dihydridobis(silyl) complex [Rh{κ²-(*N*,*N*)-(C_6F_5)*N*C(Me)CHC(Me)*N*(C_6F_5)}$(H)_2(SiMe_3)_2$] (**16**) was formed in addition to **10a**.

Introduction

Transition-metal complexes supported by β-diketiminato or β-ketiminato ligands have received increasing attention.[1–3] The versatile electronic properties and steric demands of β-diketiminates or β-ketiminates can be adjusted by variation of the substituents in the ligand backbone or at the nitrogen atoms to give access to transition-metal compounds that can exhibit unusual geometries and/or low coordination numbers.[1–3] Hence, a variety of (β-diketiminato)rhodium complexes[4–12] have been developed. For example, the complex [Rh{κ²-(*N*,*N*)-(2,6-$Me_2C_6H_3$)*N*C(Me)CHC(Me)*N*(2,6-$Me_2C_6H_3$)}(coe)] [coe = (*Z*)-cyclooctene] can be employed in the hydrogenation of olefins.[4,5] [Rh{κ²-(*N*,*N*)-(2,6-$Me_2C_6H_3$)*N*C(Me)CHC(Me)*N*(2,6-$Me_2C_6H_3$)}(coe)(N_2)] was used in the P–P activation of P_5Et_5 or P_5Ph_5.[6] The (β-diketiminato)rhodium complexes [Rh{κ²-(*N*,*N*)-(2,6-*i*$Pr_2C_6H_3$)*N*C(R)CHC(R)*N*(2,6-*i*$Pr_2C_6H_3$)}$(CO)_2$] (R = CH_3, CF_3) can be transformed into the rhodium compounds [Rh{κ²-(*N*,*N*)-(2,6-*i*$Pr_2C_6H_3$)-*N*C(R)CHC(R)*N*(2,6-*i*$Pr_2C_6H_3$)}(phdi)] (phdi = 9,10-phenanthrenediimine) in the presence of *N*,*N*′-bis(trimethylsilyl)-9,10-phenanthrenediimine and $ONMe_3$.[7] The subsequent reaction of [Rh{κ²-(*N*,*N*)-(2,6-*i*$Pr_2C_6H_3$)*N*C(R)CHC(R)-*N*(2,6-*i*$Pr_2C_6H_3$)}(phdi)] with X_2 (X = Cl, Br, I) led to the formation of *trans*-[Rh{κ²-(*N*,*N*)-(2,6-*i*$Pr_2C_6H_3$)*N*C(R)-CHC(R)*N*(2,6-*i*$Pr_2C_6H_3$)}$(X)_2$(phdi)] by oxidative addition of the halogens.[8] In the presence of [Rh{κ²-(*N*,*N*)-(2,6-*i*$Pr_2C_6H_3$)*N*C(Me)CHC(Me)*N*(2,6-*i*$Pr_2C_6H_3$)}(coe)(N_2)],[9] the heterodehydrocoupling of secondary phosphines with silanes was observed.[10] For example, the coupling of Ph_2PH and H_2SiPh_2 yielded Ph_2PSiPh_2H and dihydrogen. Mechanistic steps might include the formation of the (hydrido)(silyl)rhodium complex [Rh{κ²-(*N*,*N*)-(2,6-*i*$Pr_2C_6H_3$)*N*C(Me)CHC(Me)*N*(2,6-*i*$Pr_2C_6H_3$)}(H)($SiPh_2H$)-($PHPh_2$)], which was synthesized in an independent reaction.[10] Recently, [Rh{κ²-(*N*,*N*)-(2,6-MeC_6H_3)*N*C(Me)-CHC(Me)*N*(2,6-MeC_6H_3)}(coe)(N_2)] was applied for the Si–H activation of $HSiEt_3$.[11] In an initial step the dihydridobis(silyl)rhodium complex *cis*,*trans*-[Rh{κ²-(*N*,*N*)-(2,6-MeC_6H_3)*N*C(Me)CHC(Me)*N*(2,6-MeC_6H_3)}$(H)_2(SiEt_3)_2$] is formed. The latter is not stable in solution and quantitatively transforms into ethane and a rhodium complex, in which one $SiEt_2$ moiety is bridged to a benzylic carbon atom of the β-diketiminato ligand.[11] One step in the coupling of $HSiEt_3$ to the β-diketiminato ligand might include the cyclometallation of a benzylic C–H bond of the aryl substituent of the β-diketiminate.[3,11] To avoid cyclometallation reactions of the *N*-bound aryl rings, the choice of the substituents of the β-diketiminato ligand might therefore be critical. One option could be the use of perfluorinated groups, because the corresponding ligands do not contain

[a] Humboldt-Universität zu Berlin,
Department of Chemistry,
Brook-Taylor-Straße 2, 12489 Berlin
E-mail: thomas.braun@chemie.hu-berlin.de
http://www2.hu-berlin.de/chemie/braun/

Supporting information for this article is available on the WWW under http://dx.doi.org/10.1002/ejic.201402087.

an aryl C–H bond.[13] In addition, fluorinated ligands can have a stabilizing influence that allows the detection or even isolation of transition-metal complexes with unusual structural motifs.[14] The β-diketimine $(C_6F_5)NC(Me)CHC(Me)NH(C_6F_5)$ (**17**)[15] might, therefore, be an interesting and potent ligand precursor.[16] Herein, we report the synthesis and reactivity of a series of rhodium complexes that bear a fluorinated β-diketiminato ligand as well as a fluorinated β-ketiminato ligand. The reactivity of [Rh{κ²-(*N*,*N*)-(C_6F_5)-*N*C(Me)CHC(Me)*N*(C_6F_5)}(CO)(NCMe)] (**7a**) towards tertiary silanes was also studied.

Results and Discussion

Reaction of dipivaloylmethane with pentafluoroaniline in the presence of *para*-toluenesulfonic acid (HOTs) at 111 °C led to the formation of the β-ketimine (*t*Bu)(O)-CCH_2C(*t*Bu)N(C_6F_5) (**18**). Treatment of **18** with KH in THF at –20 °C afforded dihydrogen and the β-ketiminate [K{(*t*Bu)(O)CCHC(*t*Bu)N(C_6F_5)}] (**19**). In solution, compound **19** is stable for several hours. The rhodium derivative [Rh{κ²-(*N*,*O*)-(*t*Bu)(*O*)CCHC(*t*Bu)*N*(C_6F_5)}(cod)] (**1**) [cod = (1*Z*,5*Z*)-1,5-cyclooctadiene] was obtained by the reaction of **19** with [{Rh(μ-Cl)(cod)}$_2$] (Scheme 1).

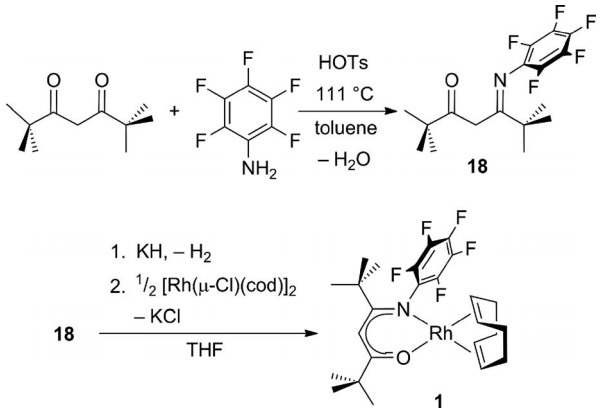

Scheme 1. Formation of (*t*Bu)(O)CCH_2C(*t*Bu)N(C_6F_5) (**18**) and [Rh{κ²-(*N*,*O*)-(*t*Bu)(*O*)CCHC(*t*Bu)*N*(C_6F_5)}(cod)] (**1**).

Deprotonation of the β-diketimine $(C_6F_5)NC(Me)CHC(Me)NH(C_6F_5)$ (**17**) with KH led to the formation of [K{(C_6F_5)NC(Me)CHC(Me)N(C_6F_5)}] (**20**), which is stable in solution for several hours. Reaction of **20** with [{Rh(μ-Cl)(cod)}$_2$] yielded [Rh{κ²(*N*,*N*)-(C_6F_5)*N*C(Me)CHC(Me)*N*(C_6F_5)}(cod)] (**2**) (Scheme 2).

The ^{1}H NMR spectrum of the β-ketimine **18** shows three singlets at δ = 1.28, 1.54, and 2.79 ppm, which were assigned to the non-equivalent *t*Bu groups and the methylene bridge between the carbonyl and the imino function, respectively. The ^{19}F NMR spectrum of **18** displays three signals at δ = –153.3, –165.9, and –166.9 ppm for the perfluorinated phenyl substituent. Resonances at δ = 207.2 and 183.9 ppm in the $^{13}C\{^1H\}$ NMR spectrum can be attributed to the carbonyl and the imino group. The solid-state IR spectrum (ATR) of **18** shows absorption bands at $\tilde{\nu}$ = 1710 and 1637 cm^{-1}, which can be assigned to the C=O and

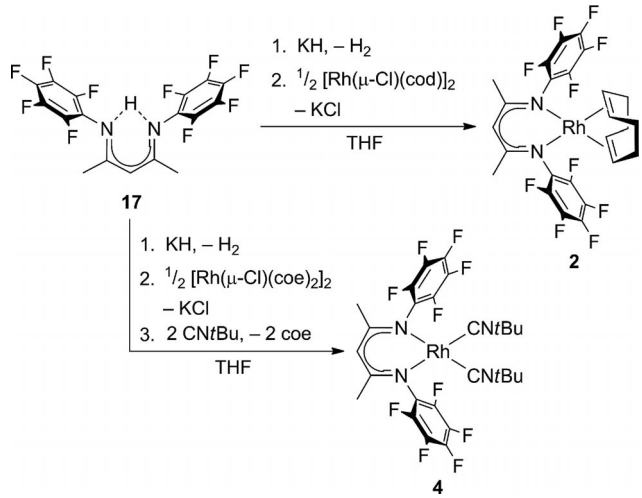

Scheme 2. Formation of [Rh{κ²(*N*,*N*)-(C_6F_5)*N*C(Me)CHC(Me)-*N*(C_6F_5)}(cod)] (**2**) and [Rh{κ²-(*N*,*N*)-(C_6F_5)*N*C(Me)CHC(Me)-*N*(C_6F_5)}$(CNtBu)_2$] (**4**).

C=N stretching vibration, respectively. The structure of **18** in the solid state was determined by X-ray crystallography (Figure 1). Selected bond lengths and angles are summarized in Table 1. The C9–O1 and the C7–N1 distances [1.206(3) and 1.277(3) Å] of the β-ketimine **18** are comparable to the data for other C=O or C=N double bonds,[17] the distances C7–C8 [1.508(3) Å] and C8–C9 [1.527(3) Å] in the ligand backbone account for C–C single bonds. The N1–C7–C8–C9 torsion angle in **18** is 77.8(3)°. In contrast, the solid-state structure of (Me)(O)CCHC(Me)NH(C_6F_5) shows a *syn* orientation of the C=O and the C–NH(C_6F_5) unit, thus designating a β-aminoenone structure.[18]

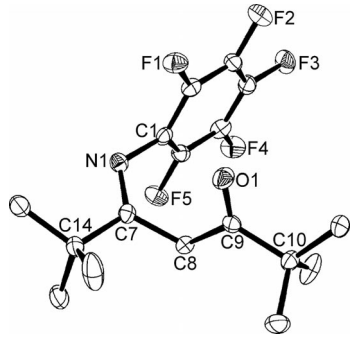

Figure 1. Molecular structure of (*t*Bu)(O)CCH_2C(*t*Bu)N(C_6F_5) (**18**) (ORTEP, ellipsoids set at 50% probability).

Table 1. Selected bond lengths [Å] and angles [°] for (*t*Bu)(O)-CCH_2C(*t*Bu)N(C_6F_5) (**18**).

C9–O1	1.206(3)	C7–C8–C9	112.79(19)
C7–N1	1.277(3)	N1–C7–C8	123.8(2)
C1–N1	1.410(3)	N1–C7–C14	119.3(2)
C9–C10	1.526(3)	C7–N1–C1	118.8(2)
C8–C9	1.527(3)	C8–C7–C14	116.9(2)
C7–C8	1.508(3)	C10–C9–C8	116.73(19)
C7–C14	1.521(3)	N1–C7–C8–C9	77.8(3)
O1–C9–C10	122.4(2)	C8–C7–N1–C1	2.0(3)
O1–C9–C8	120.9(2)	C7–C8–C9–O1	–10.3(3)

The ^{19}F NMR spectra of **19** and **20** each show three signals at δ = –157.1, –171.5, and –180.7 ppm and δ = –156.0, –168.3, and –174.3 ppm, respectively. The ^{1}H NMR spectrum of **19** displays three singlets at δ = 5.46, 1.54, and 1.22 ppm, which were assigned to the methine proton and the inequivalent *t*Bu groups in the ligand backbone. The methine proton and the methyl groups in the ligand backbone of **20** afforded two singlets at δ = 4.86 and 1.74 ppm.

Complexes **1** and **2** are soluble in benzene, toluene, or THF, slightly soluble in hexane, pentane, or Et_2O, and are inert to water, dioxygen, or dihydrogen. The ^{19}F NMR spectra feature three signals for the perfluorinated phenyl substituent at δ = –144.6, –161.3, and –164.0 ppm, which integrate in a ratio of 2:1:2 (for **1**) and at δ = –147.8, –159.0, and –162.9 ppm with an integral ratio of 2:1:2 (for **2**). Three singlet resonances in the ^{1}H NMR spectrum of **1** at δ = 5.76, 1.13, and 0.94 ppm can be assigned to the methine proton and the inequivalent *t*Bu groups in the backbone of the β-ketiminato ligand. In the ^{1}H NMR spectrum of **2**, the methine proton and the methyl groups in the ligand backbone cause two singlets at δ = 4.98 and 1.38 ppm, respectively. Multiplets at δ = 4.57, 2.71, 2.21, and 1.49 ppm can be attributed to the olefinic protons and the CH_2 groups of the cod ligand in **1**.[5] The cod ligand of complex **2** affords resonance signals at δ = 3.31 ppm for the olefinic protons and signals at δ = 1.96 and 1.38 ppm for the CH_2 groups.[5,9] The structures of **1** and of **2** in the solid state were determined by X-ray crystallography (Figure 2). Selected bond lengths and angles are summarized in Tables 2 and 3.

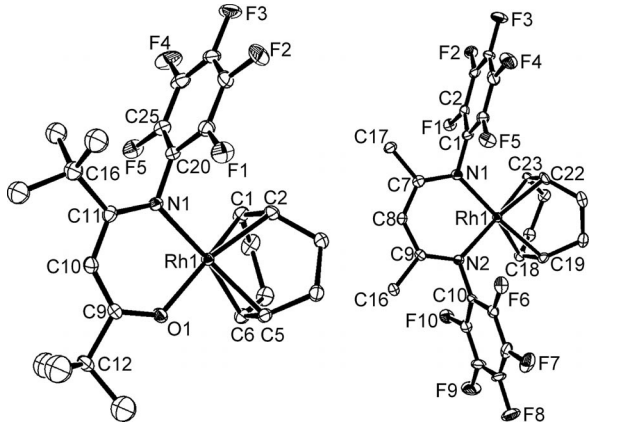

Figure 2. Molecular structures of [Rh{κ²-(*N*,*O*)-(*t*Bu)(*O*)-CCHC(*t*Bu)*N*(C_6F_5)}(cod)] (**1**) (left) and [Rh{κ²(*N*,*N*)-(C_6F_5)-*N*C(Me)CHC(Me)*N*(C_6F_5)}(cod)] (**2**) (ORTEP, ellipsoids set at 50% probability).

If the cod ligand is considered to be a bidentate ligand that occupies two coordination sites, both structures are approximately square-planar. The O1–Rh1–N1 angle of **1** is 89.88(7)°. The N1–Rh1 and the O1–Rh1 distances in **1**, Rh1–N1 and Rh1–N2 in complex **2**, as well as the average Rh–C_{cod} distances (**1**: 2.125 Å; **2**: 2.144 Å) are in good agreement with the separations in related complexes.[5,9,19] The distances in the backbones of the fluorinated ligands as well as the small torsion angles [**1**: C9–C10–C11–N1 5.4(4)°; **2**: N1–C7–C8–C9 6.48(12)°] suggest the presence of

Table 2. Selected bond lengths [Å] and angles [°] for [Rh{κ²-(*N*,*O*)-(*t*Bu)(*O*)CCHC(*t*Bu)*N*(C_6F_5)}(cod)] (**1**).

N1–Rh1	2.1187(19)	C1–Rh1–C6	81.73(9)
O1–Rh1	2.0156(16)	C1–Rh1–N1	97.69(8)
C1–Rh1	2.104(2)	O1–Rh1–C6	84.07(8)
C2–Rh1	2.136(2)	O1–Rh1–N1	89.88(7)
C5–Rh1	2.123(2)	C9–O1–Rh1	127.57(15)
C6–Rh1	2.138(2)	C11–N1–Rh1	125.10(15)
C1–C2	1.400(4)	C20–N1–Rh1	114.02(14)
C5–C6	1.397(3)	C11–N1–C20	120.85(19)
C11–N1	1.347(3)	O1–C9–C10	125.6(2)
C20–N1	1.414(3)	N1–C11–C10	121.4(2)
C9–O1	1.267(3)	C25–C20–N1–Rh1	–91.1(3)
C9–C10	1.391(3)	C10–C9–O1–Rh1	–6.3(4)
C10–C11	1.402(3)	C9–C10–C11–N1	5.4(4)
C9–C12	1.538(3)	C10–C11–N1–C20	177.2 (2)
C11–C16	1.566(3)		

Table 3. Selected bond lengths [Å] and angles [°] for [Rh{κ²(*N*,*N*)-(C_6F_5)*N*C(Me)CHC(Me)*N*(C_6F_5)}(cod)] (**2**).

Rh1–N1	2.090(2)	C9–C16	1.513(3)
Rh1–N2	2.104(2)		
Rh1–C18	2.133(2)	N2–Rh1–N1	88.40(8)
Rh1–C22	2.133(2)	N2–Rh1–C18	91.33(9)
Rh1–C23	2.148(2)	N1–Rh1–C22	93.86(9)
Rh1–C19	2.162(2)	N1–C7–C8	124.3(2)
C18–C19	1.397(4)	N1–C7–C17	120.3(2)
C22–C23	1.390(4)	C9–C8–C7	129.0(2)
N1–C1	1.420(3)	C9–N2–Rh1	125.81(16)
N1–C7	1.335(3)	C7–N1–Rh1	124.41(16)
N2–C10	1.422(3)	N1–C7–C8–C9	6.48(12)
N2–C9	1.338(3)	C1–N1–C7–C8	–172.16(12)
C7–C8	1.399(3)	C2–C1–N1–C7	96.79(14)
C8–C9	1.388(3)	Rh1–N1–C7–C8	13.3(2)
C7–C17	1.511(3)		

almost planar π systems.[19] In both compounds the perfluorinated aryl substituents are to some extent in an orthogonal orientation to the ligand backbone, which is shown by the angles C25–C20–N1–Rh1 of –91.1(3)° in complex **1** and C2–C1–N1–C7 of 96.79(14)° in **2**.

The ethylene complex [Rh{κ²-(*N*,*N*)-(C_6F_5)*N*C(Me)-CHC(Me)*N*(C_6F_5)}(C_2H_4)$_2$] (**3**) can be synthesized by adding **20** to a solution of [{Rh(μ-Cl)(C_2H_4)$_2$}$_2$]. The ^{1}H NMR spectrum of **3** displays resonances at δ = 2.45 and 1.73 ppm, which can be attributed to the ethylene ligands. The $^{13}C\{^{1}H\}$ NMR spectrum features a doublet at δ = 61.5 ppm for the carbon atoms of the ethylene ligands with a rhodium–carbon coupling constant of $J_{Rh,C}$ = 12.4 Hz. The ^{19}F NMR spectrum of **3** reveals three signals for both perfluorinated phenyl substituents at δ = –147.2, –158.2, and –162.9 ppm with an integral ratio of 2:1:2. In the liquid injection field desorption ionization time-of-flight (LIFDI TOF) mass spectrum, a peak with *m*/*z* = 588.2 can be attributed to the molecule ion [Rh{κ²-(*N*,*N*)-(C_6F_5)*N*C(Me)-CHC(Me)*N*(C_6F_5)}(C_2H_4)$_2$]$^+$. Complex **3** can be stored for some days under ethylene at –30 °C but decomposes within hours at room temperature.

The formal oxidation state of metal centers in transition-metal complexes that contain π-accepting ligands such as carbonyl[7,12a,20,21] or isocyanido ligands[22–24] can be esti-

mated by characteristic absorption bands of these π-acceptor ligands in the IR or Raman spectra. The use of such ligands might therefore provide a helpful tool to obtain information on the electronic properties of the metal center. Treatment of [{Rh(μ-Cl)(coe)$_2$}$_2$] with **20** followed by addition of CN*t*Bu led to the formation of [Rh{κ^2-(*N*,*N*)-(C_6F_5)*N*C(Me)CHC(Me)*N*(C_6F_5)}(CN*t*Bu)$_2$] (**4**) (Scheme 2). The solid-state IR spectrum of **4** shows three absorption bands at $\tilde{\nu}$ = 2137, 2094, and 2064 cm^{-1} for two CN*t*Bu ligands at a rhodium(I) complex.[22–24] Spectra measured in toluene and THF also reveal three bands at $\tilde{\nu}$ = 2137, 2095, and 2061 cm^{-1} (toluene) and at $\tilde{\nu}$ = 2139, 2096, and 2061 cm^{-1} (THF). However, DFT calculations to model the IR spectrum of **4** in the gas phase show only two absorption bands at $\tilde{\nu}$ = 2189 and 2133 cm^{-1} (B3LYP/cc-pvdz). The occurrence of three isocyanide bands might be due to intermolecular interactions in the liquid and in the solid state, which lower the symmetry of the compound relative to the isolated gaseous phase.[24d,24e] The presence of three absorption bands in the IR spectra of diisonitrile complexes has been documented in the literature.[24] The $^{13}C\{^1H\}$ NMR spectrum exhibits an unusually high-field-shifted[22] doublet resonance for the rhodium-bound carbon atoms at δ = 147.8 ppm with a rhodium–carbon coupling constant of $^1J_{Rh,C}$ = 65.1 Hz. The structure of **4** in the solid state was determined by X-ray crystallography (Figure 3); selected bond lengths and angles are summarized in Table 4. The rhodium atom in **4** exhibits again a square-planar coordination sphere. The rhodium–carbon distances are 1.893(2) and 1.893(3) Å, and the carbon–nitrogen distances in the isocyanido ligands are 1.155(3) and 1.161(3) Å. These values are comparable to the data in other isocyanide complexes.[22–24] The rhodium isocyanide units exhibit angles of Rh1–C18–N3 177.5(2)° and Rh1–C23–N4 176.6(2)°.

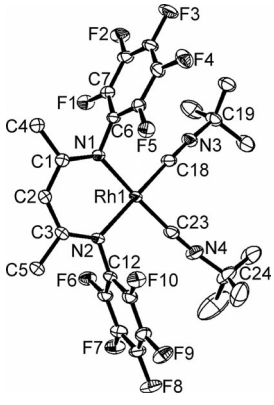

Figure 3. Molecular structure of [Rh{κ^2-(*N*,*N*)-(C_6F_5)*N*C(Me)CHC(Me)*N*(C_6F_5)}(CN*t*Bu)$_2$] (**4**) (ORTEP, ellipsoids set at 50% probability).

Comparable structural and spectroscopic data can be found for the non-fluorinated complex [Rh{κ^2(*N*,*N*)-(2,6-$Me_2C_6H_3$)*N*-C(Me)CHC(Me)*N*(2,6-$Me_2C_6H_3$)}(CN*t*Bu)$_2$] (**5**). Complex **5** is accessible by treatment of [{Rh(μ-Cl)(coe)$_2$}$_2$] with [Li{(2,6-$Me_2C_6H_3$)NC(Me)CHC(Me)N(2,6-$Me_2C_6H_3$)}] followed by the addition of CN*t*Bu. The presence of a rhodium(I) complex is again evidenced by absorption bands at $\tilde{\nu}$ = 2140, 2103, and 2068 cm^{-1} for two CN*t*Bu ligands in the IR spectrum (ATR).[22–24] The $^{13}C\{^1H\}$-NMR spectrum features a doublet resonance signal at δ = 150.5 ppm with a rhodium–carbon coupling constant of $^1J_{Rh,C}$ = 63.0 Hz. The structure of **5** in the solid state was also determined by X-ray crystallography (Figure 4); selected bond lengths and angles are summarized in Table 5. The distances Rh1–N1 [2.0727(13) Å] and Rh1–N2 [2.0672(14) Å] in **5** are comparable to those found in **4**.

Table 4. Selected bond lengths [Å] and angles [°] for [Rh{κ^2-(*N*,*N*)-(C_6F_5)*N*C(Me)CHC(Me)*N*(C_6F_5)}(CN*t*Bu)$_2$] (**4**).

Rh1–N1	2.0738(19)	C2–C3	1.396(3)
Rh1–N2	2.0671(18)		
Rh1–C18	1.893(2)	N1–Rh1–N2	88.40(7)
Rh1–C23	1.892(3)	N2–Rh1–C18	176.36(10)
C18–N3	1.154(3)	N1–Rh1–C23	176.09(10)
C23–N4	1.163(3)	C18–Rh1–C23	84.92(10)
C1–C2	1.397(3)	C1–C2–C3	128.3(2)
N1–C1	1.327(3)	Rh1–C18–N3	177.6(2)
N1–C6	1.420(3)	Rh1–C23–N4	176.6(2)
N2–C3	1.327(3)	N1–C1–C2–C3	6.1(5)
N2–C12	1.416(3)	C6–N1–C1–C2	–173.1(3)
N3–C19	1.455(3)	C7–C6–N1–C1	–86.3(3)
N4–C24	1.443(4)		

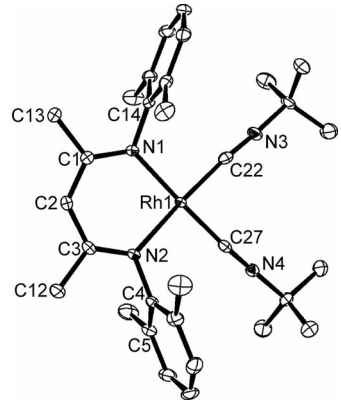

Figure 4. Molecular structure of [Rh{κ^2(*N*,*N*)-(2,6-$Me_2C_6H_3$)-*N*C(Me)CHC(Me)*N*(2,6-$Me_2C_6H_3$)}(CN*t*Bu)$_2$] (**5**) (ORTEP, ellipsoids set at 50% probability).

Table 5. Selected bond lengths [Å] and angles [°] for [Rh{κ^2(*N*,*N*)-(2,6-$Me_2C_6H_3$)*N*C(Me)CHC(Me)*N*(2,6-$Me_2C_6H_3$)}(CN*t*Bu)$_2$] (**5**).

Rh1–N1	2.0727(13)	C2–C3	1.397(2)
Rh1–N2	2.0672(14)		
Rh1–C22	1.8951(17)	N1–Rh1–N2	90.38(5)
Rh1–C27	1.9048(17)	N2–Rh1–C22	176.35(6)
C22–N3	1.158(2)	N1–Rh1–C27	176.40(6)
C27–N4	1.158(2)	C22–Rh1–C27	84.70(7)
C1–C2	1.399(2)	C1–C2–C3	128.86(16)
N1–C1	1.328(2)	Rh1–C22–N3	175.50(15)
N1–C14	1.435(2)	Rh1–C27–N4	175.52(15)
N2–C3	1.325(2)	N1–C1–C2–C3	5.76(28)
N2–C4	1.435(2)	C4–N2–C3–C2	173.92(17)
N3–C23	1.450(2)	C5–C4–N2–C3	91.60(11)
N4–C28	1.454(2)		

Treatment of the dinuclear complex [{Rh(μ-Cl)(CO)$_2$}$_2$] with **20** led to the formation of [Rh{κ^2(*N*,*N*)-(C_6F_5)*N*C-

(Me)CHC(Me)$N(C_6F_5)$}$(CO)_2$] (**6a**) (Scheme 3). The isotopologue [Rh{κ²(*N*,*N*)-(C_6F_5)*N*C(Me)CHC(Me)$N(C_6F_5)$}-$(^{13}CO)_2$] (**6b**) is available in a similar fashion from [{Rh(μ-Cl)$(^{13}CO)_2$}$_2$]. In addition, 2,3,4,5,6-pentafluoro-*N*-[(*Z*)-6,7,8,9-tetrafluoro-2-methyl-1*H*-benzo[*b*]azepine-4(5*H*)-ylidene]benzeneamine (**22**) can be isolated as a byproduct (see the Supporting Information). The presence of a rhodium(I) complex is evidenced by two characteristic absorption bands at $\tilde{\nu}$ = 2070 and 2020 cm^{-1} in the IR spectrum (ATR) of **6a**, which can be assigned to the symmetric and asymmetric CO stretching vibration of the carbonyl ligands.[7,12a,20,21] For **6b**, these bands shift to $\tilde{\nu}$ = 2022 and 1975 cm^{-1}, respectively. The structurally related complex [Rh{κ²-(*N*,*N*)-(2,6-*i*Pr$_2$C$_6$H$_3$)*N*C(CF$_3$)CHC(CF$_3$)*N*(2,6-*i*Pr$_2$C$_6$H$_3$)}(CO)$_2$] bears electron-withdrawing CF$_3$ groups in the backbone of the β-diketiminato ligand and shows absorption bands at $\tilde{\nu}$ = 2078 and 2020 cm^{-1},[7] which are in the same range as for **6a**. In contrast to these fluorinated β-diketiminato complexes, [Rh{κ²-(*N*,*N*)-(2,6-*i*Pr$_2$C$_6$H$_3$)*N*C-(CH$_3$)CHC(CH$_3$)*N*(2,6-*i*Pr$_2$C$_6$H$_3$)}(CO)$_2$] exhibits bands at $\tilde{\nu}$ = 2053 and 1988 cm^{-1}.[7] Thus, the perfluorinated aryl groups in **6a** decrease the electron density at the rhodium center in comparison to non-fluorinated complexes. A doublet signal at δ = 184.4 ppm in the $^{13}C\{^1H\}$ NMR spectrum with a rhodium–carbon coupling constant of $^1J_{Rh,C}$ = 66.6 Hz is assigned to the carbonyl ligands in **6b**. The other NMR spectroscopic data of **6a** and **6b** are as expected.

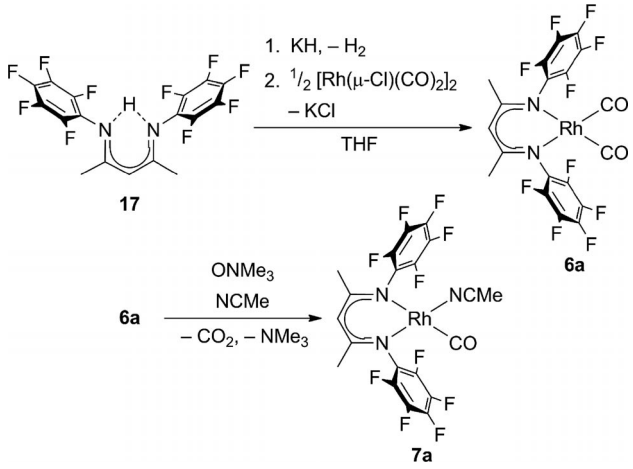

Scheme 3. Formation of [Rh{κ²(*N*,*N*)-(C_6F_5)*N*C(Me)CHC(Me)-$N(C_6F_5)$}$(CO)_2$] (**6a**) and [Rh{κ²-(*N*,*N*)-(C_6F_5)*N*C(Me)CHC(Me)-$N(C_6F_5)$}(CO)(NCMe)] (**7a**).

The structure of **6a** in the solid state was also determined by X-ray crystallography (Figure 5). Selected bond lengths and angles are summarized in Table 6. In the solid state the rhodium atom in **6a** adopts a square-planar coordination sphere. The Rh1–N1 [2.0565(18) Å] and Rh1–N2 [2.0517(17) Å] distances in **6a** are slightly shortened relative to **2** or **4** but are in good agreement with the distances found in [Rh{κ²-(*N*,*N*)-(2,6-*i*Pr$_2$C$_6$H$_3$)*N*C(CH$_3$)CHC(CH$_3$)-*N*(2,6-*i*Pr$_2$C$_6$H$_3$)}(CO)$_2$] [2.0514(11) and 2.0491(11) Å].[7] Both the rhodium–carbon distances [1.871(3) and 1.864(3) Å] and the carbon–oxygen bond lengths [1.129(3) and 1.124(3) Å] of the carbonyl ligands are in accordance with the data for (carbonyl)transition-metal complexes[20,21] {e.g., [Rh{κ²-(*N*,*N*)-(2,6-*i*Pr$_2$C$_6$H$_3$)*N*C(CH$_3$)CHC(CH$_3$)-*N*(2,6-*i*Pr$_2$C$_6$H$_3$)}(CO)$_2$], 1.1358(18) and 1.1365(17) Å}.[7]

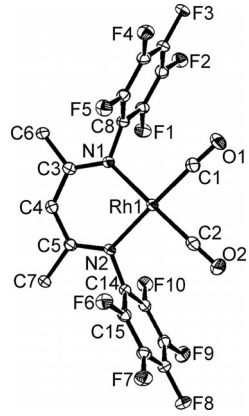

Figure 5. Molecular structure of [Rh{κ²(*N*,*N*)-(C_6F_5)*N*C(Me)-CHC(Me)$N(C_6F_5)$}$(CO)_2$] (**6a**) (ORTEP, ellipsoids set at 50% probability).

Table 6. Selected bond lengths [Å] and angles [°] for [Rh{κ²(*N*,*N*)-(C_6F_5)*N*C(Me)CHC(Me)$N(C_6F_5)$}$(CO)_2$] (**6a**).

Rh1–N1	2.0565(18)	N1–Rh1–N2	88.91(7)
Rh1–N2	2.0517(17)	N2–Rh1–C1	178.08(9)
Rh1–C1	1.871(3)	N1–Rh1–C2	178.77(10)
Rh1–C2	1.864(3)	C1–Rh1–C2	85.98(11)
C1–O1	1.129(3)	C3–C4–C5	128.3(2)
C2–O2	1.124(3)	Rh1–C1–O1	178.4(2)
N1–C3	1.333(3)	Rh1–C2–O2	179.0(3)
N1–C8	1.422(3)	N1–C3–C4–C5	–3.4(4)
N2–C5	1.332(3)	C1–Rh1–N1–C8	4.50(17)
N2–C14	1.423(3)	C15–C14–N2–C5	–86.9(2)
C3–C4	1.399(3)		
C4–C5	1.398(3)		

Complexes **4**, **5**, and **6a** are inert toward dioxygen or water. However, treatment of **6a** with $ONMe_3$ in the presence of acetonitrile gave NMe_3, CO_2, and [Rh{κ²-(*N*,*N*)-(2,6-MeC$_6$H$_3$)*N*C(Me)CHC(Me)*N*(2,6-MeC$_6$H$_3$)}(CO)-(NCMe)] (**7a**) (Scheme 3). The ^{13}C-labeled isotopomer [Rh{κ²(*N*,*N*)-(C_6F_5)*N*C(Me)CHC(Me)$N(C_6F_5)$}(^{13}CO)-(NCMe)] (**7b**) is available from **6b** in a similar fashion. The presence of a rhodium(I) complex **6a** is evidenced by an absorption band in the solid-state IR spectrum of **7a** at $\tilde{\nu}$ = 1992 cm^{-1}, which can be attributed to the stretching vibration of the carbonyl ligand.[7,12a,20,21] This band shifts to $\tilde{\nu}$ = 1946 cm^{-1} for the ^{13}C-labeled complex **7b**. A weak absorption band at $\tilde{\nu}$ = 2283 cm^{-1} can be assigned to the NCMe ligand. For comparison, the cationic compound $[Rh(CO)_2(NCMe)_2]^+$ shows two bands at $\tilde{\nu}$ = 2330 and 2300 cm^{-1} for the NCMe ligand. In (acetonitrile)rhodium(III) complexes, stretching vibrations were found at $\tilde{\nu}$ = 2360 cm^{-1}.[25] The lower energy of the absorption band that is assigned to the stretching vibration of the carbonyl ligand in **7a** ($\tilde{\nu}$ = 1992 cm^{-1}) relative to **6a** ($\tilde{\nu}$ = 2070 and 2020 cm^{-1}) and the downfield shift of the $^{13}C\{^1H\}$ resonance signal for the CO carbon atom (δ = 188.8 ppm for

7a relative to δ = 184.4 ppm for **6a**) indicate a stronger π backbonding in **7a**.[7,20,21,26] In contrast to complex **6a**, the ^{19}F NMR spectrum of **7a** displays six resonance signals, which is a result of the different ligands in the *trans* position to the β-diketiminato ligand. The $^{13}C\{^{1}H\}$ NMR spectrum of **7b** features a doublet resonance for the carbonyl ligand at δ = 188.8 ppm with a rhodium–carbon coupling constant of $^{1}J_{Rh,C}$ = 71.5 Hz.

Figure 6 shows the solid-state structure of **7a**, which was determined by X-ray crystallography. Selected bond lengths and angles are summarized in Table 7. Compound **7a** adopts a square-planar coordination sphere. The Rh1–N1 distance of 2.019(3) Å is shortened relative to Rh1–N2 [2.059(12) Å]. The latter moiety is located in the *trans* position to the carbonyl ligand. This observation reflects the stronger π-acceptor properties of the CO ligand relative to the coordinated acetonitrile. The Rh1–C20 distance amounts to 1.825(3) Å, and comparable separations can be found in other (carbonyl)transition-metal complexes.[7,20,21] The CO distance in the carbonyl ligand is with 1.152(4) Å slightly longer than those found in **6a** (average of 1.127 Å) or [Rh{κ^2-(*N*,*N*)-(2,6-*i*Pr$_2$C$_6$H$_3$)*N*C(Me)CHC(Me)*N*(2,6-*i*Pr$_2$C$_6$H$_3$)}(CO)$_2$][7] (average 1.136 Å).

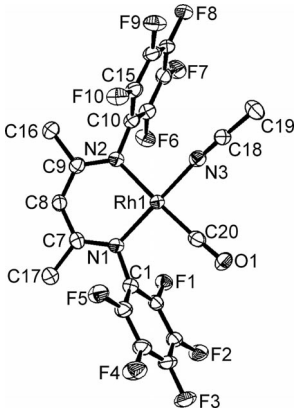

Figure 6. Molecular structure of [Rh{κ^2-(*N*,*N*)-(C$_6$F$_5$)*N*C(Me)CHC(Me)*N*(C$_6$F$_5$)}(CO)(NCMe)] (**7a**) (ORTEP, ellipsoids set at 50% probability).

Table 7. Selected bond lengths [Å] and angles [°] for [Rh{κ^2-(*N*,*N*)-(C$_6$F$_5$)*N*C(Me)CHC(Me)*N*(C$_6$F$_5$)}(CO)(NCMe)] (**7a**).

Rh1–N1	2.019(3)	N1–Rh1–N2	89.95(10)
Rh1–N2	2.059(2)	C20–Rh1–N3	86.14(13)
Rh1–N3	2.011(3)	N1–Rh1–N3	174.64(10)
Rh1–C20	1.825(3)	C20–Rh1–N2	176.47(13)
O1–C20	1.152(4)	C1–N1–Rh1	115.1(2)
N3–C18	1.142(4)	O1–C20–Rh1	176.3(3)
C18–C19	1.449(5)	Rh1–N3–C18	170.0(3)
N1–C1	1.423(4)	N3–C18–C19	178.2(3)
N2–C10	1.418(4)	C9–N2–C10–C15	91.2(4)
N1–C7	1.340(4)	C20–Rh1–N3–C18	–42.3(17)
N2–C9	1.342(4)	N1–C7–C8–C9	6.0(5)
C7–C8	1.399(4)	Rh1–N1–C7–C8	6.4(5)
C8–C9	1.385(5)		
C7–C17	1.496(5)		

Complex **7a** shows no reaction with ONMe$_3$, and a reaction of both CO ligands in **6a** in the presence of an excess amount of ONMe$_3$ was also not observed. This observations are in contrast to the reactivity of [Rh{κ^2-(*N*,*N*)-(2,6-*i*Pr$_2$C$_6$H$_3$)*N*C(Me)CHC(Me)*N*(2,6-*i*Pr$_2$C$_6$H$_3$)}(CO)$_2$][7] However, we were able to identify [Rh{κ^2(*N*,*N*)-(C$_6$F$_5$)-*N*C(Me)CHC(Me)*N*(C$_6$F$_5$)}(CO)(NMe$_3$)] (**23**) by using 1,2-difluorobenzene as the solvent instead of acetonitrile. Complex **23** is presumably an intermediate in the formation of **7a** and is the initial product formed prior to the coordination of the acetonitrile to give **7a**. Complex **23** could only be characterized by NMR spectroscopy in solution due to decomposition upon evaporation of the solvent 1,2-C$_6$H$_4$F$_2$. However, an absorption band for the CO stretching vibration at $\tilde{\nu}$ = 1954 cm^{-1} in the IR spectrum of **23** (ATR), which was measured after slow evaporation of the solvent at ambient pressure, gives evidence for the presence of a rhodium(I) complex.

Acetonitrile ligands are often bound labile and can easily be replaced by other ligands.[27] Accordingly, exposure of a solution of **7a** to carbon monoxide led to the formation of **6a**. Treatment of **7a** with PEt$_3$ or NH$_3$ gave the complexes [Rh{κ^2-(*N*,*N*)-(C$_6$F$_5$)*N*C(Me)CHC(Me)*N*(C$_6$F$_5$)}(CO)-(PEt$_3$)] (**8a**) or [Rh{κ^2-(*N*,*N*)-(C$_6$F$_5$)*N*C(Me)CHC(Me)-*N*(C$_6$F$_5$)}(CO)(NH$_3$)] (**9a**), respectively (Scheme 4). The ^{13}C-labeled isotopomers [Rh{κ^2-(*N*,*N*)-(C$_6$F$_5$)*N*C(Me)-CHC(Me)*N*(C$_6$F$_5$)}(^{13}CO)(PEt$_3$)] (**8b**) or [Rh{κ^2-(*N*,*N*)-(C$_6$F$_5$)*N*C(Me)CHC(Me)*N*(C$_6$F$_5$)}(^{13}CO)(NH$_3$)] (**9b**) are available from **7b** in a similar fashion. The complexes **8a** and **9a** could only be characterized in solution owing to decomposition upon evaporation of the solvent. We did not observe any oxidative addition of an N–H bond in **9a** as was observed for other rhodium and iridium complexes.[28]

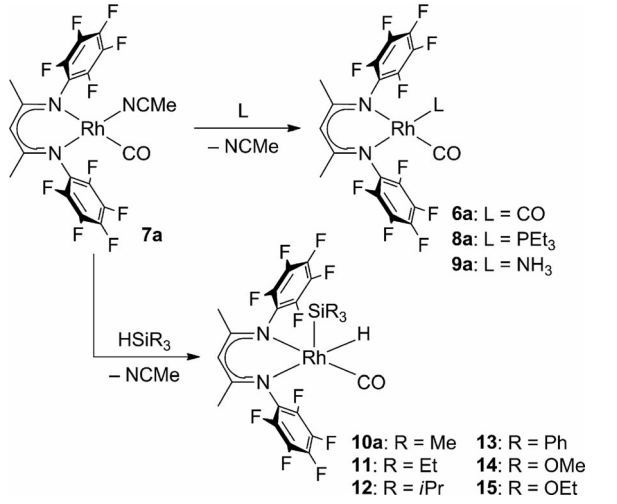

Scheme 4. Reactivity of [Rh{κ^2-(*N*,*N*)-(C$_6$F$_5$)*N*C(Me)CHC(Me)-*N*(C$_6$F$_5$)}(CO)(NCMe)] (**7a**) towards CO, PEt$_3$, NH$_3$, and HSiR$_3$ (R = Me, Et, *i*Pr, Ph, OMe, OEt).

The $^{31}P\{^{1}H\}$ NMR spectrum of **8a** displays a doublet at δ = 21.7 ppm with a rhodium–phosphorus coupling constant of $^{1}J_{Rh,P}$ = 125.8 Hz consistent with a phosphine ligand at a rhodium(I) center.[29] For **8b** the $^{31}P\{^{1}H\}$ NMR spectrum reveals a carbon–phosphorus coupling constant of $^{2}J_{P,C}$ = 17.5 Hz, which indicates a *cis* geometry of the

carbonyl and phosphine ligand.[30] A signal at δ = 191.9 ppm in the $^{13}C\{^1H\}$ NMR spectrum of **8b** can be attributed to the carbon atom of the carbonyl ligand.[7,20,21,26] The presence of the rhodium(I) complex **8a** is evidenced by an absorption band at $\tilde{\nu}$ = 1962 cm^{-1}, which can be assigned to the stretching vibration of the CO ligand.[7,12a,20,21] This band shifts to $\tilde{\nu}$ = 1914 cm^{-1} for the ^{13}C-labeled complex **8b**. The IR spectrum (ATR) of **9a** shows an absorption band at $\tilde{\nu}$ = 1956 cm^{-1} for the CO ligand, which shifts to $\tilde{\nu}$ = 1910 cm^{-1} for **9b**. Bands at $\tilde{\nu}$ = 3372 and 3364 cm^{-1} can be attributed to N–H stretching vibrations of the ammine ligand. The ^1H NMR spectrum of **9a** reveals a resonance for the NH_3 ligand at δ = 0.62 ppm. A doublet resonance signal for the CO carbon atom can be found at δ = 190.5 ppm in the $^{13}C\{^1H\}$ NMR spectrum of **9b**.

Reactions of the (β-diketiminato)rhodium complex **7a** with silanes $HSiR_3$ (R = Me, Et, *i*Pr, Ph, OMe, OEt) led to the formation of the (hydrido)(silyl)rhodium complexes [Rh{κ^2-(*N*,*N*)-(C_6F_5)*N*C(Me)CHC(Me)*N*(C_6F_5)}(H)(SiR_3)(CO)] (**10a**: R = Me; **11**: R = Et; **12**: R = *i*Pr; **13**: R = Ph; **14**: R = OMe; **15**: R = OEt) by oxidative addition (Scheme 4). The (hydrido)(silyl)rhodium complexes could not be isolated and were characterized by NMR spectroscopy only. In each case the ^1H NMR spectra show a characteristic doublet signal for the hydrido ligand[11,31] between δ = –11 and –13 ppm with a rhodium–hydrogen coupling constant ($^1J_{Rh,H}$) between 19 and 24 Hz.

An excess amount of $HSiMe_3$ led to full conversion of **7a** after 5 h and to the formation of [Rh{κ^2-(*N*,*N*)-(C_6F_5)*N*C(Me)CHC(Me)*N*(C_6F_5)}(H)($SiMe_3$)(CO)] (**10a**) as well as of [Rh{κ^2-(*N*,*N*)-(C_6F_5)*N*C(Me)CHC(Me)*N*(C_6F_5)}(H)$_2$($SiMe_3$)$_2$] (**16**) (Scheme 5). We were not able to separate compounds **10a** and **16**, in part because of the incipient formation of small amounts of (C_6F_5)NC(Me)CHC(Me)NH(C_6F_5) (**17**). Integration of the ^1H and ^{19}F NMR signals shows for **10a/16/17** a ratio of 12:1:1 after 4 h. By increasing the reaction time to 8 h, the product ratio **10a/16/17** changes to 5:2:3. Treatment of a solution of **7b** with $HSiMe_3$ gave the ^{13}C-labeled complex [Rh{κ^2-(*N*,*N*)-(C_6F_5)*N*C(Me)CHC(Me)*N*(C_6F_5)}(H)($SiMe_3$)(^{13}CO)] (**10b**) and again the dihydridobis(silyl) complex **16**.

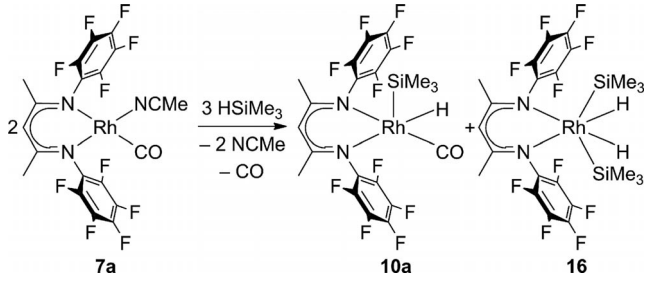

Scheme 5. Formation of Rh{κ^2-(*N*,*N*)-(C_6F_5)*N*C(Me)CHC(Me)*N*(C_6F_5)}(H)($SiMe_3$)(CO) (**10a**) and [Rh{κ^2-(*N*,*N*)-(C_6F_5)*N*C(Me)CHC(Me)*N*(C_6F_5)}(H)$_2$($SiMe_3$)$_2$] (**16**).

The reaction of **7a** with $HSiMe_3$ can be monitored by NMR spectroscopy. Initially, **10a** is formed, followed by the formation of the dihydridobis(silyl) complex **16**. In the ^1H NMR spectra a singlet at δ = 0.58 ppm can be attributed to free acetonitrile.[32] When the ^{13}C-labeled complex **7b** is used as a starting compound, a resonance signal at δ = 181.5 ppm emerged in the $^{13}C\{^1H\}$ NMR spectrum simultaneously with the formation of **16**. The signal can be attributed to ^{13}CO.[33] Treatment of the reaction mixture that consisted of **10a** and **16** with an excess amount of CO led to the formation of $HSiMe_3$[34] and **6a**.

The ^1H NMR spectrum of **10a** displays resonance signals at δ = 0.31 and –12.34 ppm, which can be assigned to the $SiMe_3$ ligand and the hydrido ligand, respectively. The doublet signal for the latter shows a rhodium–hydrogen coupling constant of $^1J_{Rh,H}$ = 22.2 Hz. The signal for the hydrido ligand in the ^{13}C-labeled complex **10b** reveals a carbon–hydrogen coupling constant of $^2J_{C,H}$ = 9.5 Hz, which is characteristic of a mutual *cis* geometry of the hydrido and the carbonyl ligand.[30] A doublet resonance in the $^{13}C\{^1H\}$ NMR spectrum of **10b** at δ = 188.2 ppm with a rhodium–carbon coupling constant of $^1J_{Rh,C}$ = 67.1 Hz can be attributed to the carbon atom of the CO ligand. The presence of a rhodium(III) complex is again evidenced by an absorption band in the IR spectrum (ATR) of **10a** at $\tilde{\nu}$ = 2072 cm^{-1}.[7,12a,20,21] This band shifts to $\tilde{\nu}$ = 2022 cm^{-1} for the ^{13}C-labeled complex **10b**. Absorption bands at $\tilde{\nu}$ = 2025 and 2017 cm^{-1} can tentatively be assigned to stretching vibrations of the Rh–H moieties of **10a** and **16**.[31] The spectroscopic data of [Rh{κ^2-(*N*,*N*)-(C_6F_5)*N*C(Me)CHC(Me)*N*(C_6F_5)}(H)$_2$($SiMe_3$)$_2$] (**16**) indicate the presence of equivalent pentafluorophenyl groups. The ^{19}F NMR spectrum of **16** displays three signals at δ = –147.6, –161.6, and –163.4 ppm. The resonance signals in the ^1H NMR spectrum at δ = 0.29 and –14.50 ppm reveal the presence of the $SiMe_3$ ligands and the hydrido ligands. The latter signal appears as a doublet with a rhodium–hydrogen coupling of $^1J_{Rh,H}$ = 23.4 Hz. The resonance correlates to a signal for the $SiMe_3$ ligands at δ = 35.5 ppm in the ^{29}Si domain in an $^1H,^{29}Si$ heteronuclear multiple-bond correlation (HMBC) NMR spectrum (Figure 7).[11,31] The NMR spectroscopic data are in accordance with those found for other bis(silyl)-rhodium(V) complexes, in which the silyl ligands are in a mutual *trans* orientation.[35]

DFT calculations were performed to model conceivable configurations of **10a** and **16**. They revealed that the isomer of [Rh{κ^2-(*N*,*N*)-(C_6F_5)*N*C(Me)CHC(Me)*N*(C_6F_5)}(H)($SiMe_3$)(CO)] (**10a**), which exhibits a mutual *cis* orientation of the hydrido and the carbonyl ligands and in which the silyl ligand occupies the apical position in a square-pyramidal complex, is the only isomer that converged to a stable structure (Figure 8; see the Supporting Information). Such a geometry with the silyl ligand in the apical position can also be found for [Rh{κ^2-(*N*,*N*)-3,5-diphenyl-2-(2-pyridyl)-pyrrolido}(H)($SiPh_3$)(PPh_3)][35] and *trans*-[Os(SiR_3)(Cl)(CO)(PPh_3)$_2$][36a] (R = F, Cl, OH, Me). The calculations also revealed that the dihydridobis(silyl) isomer **16** with a mutual *cis* orientation of the hydrido ligands is again the only isomer that converged to a stable structure (Si–Rh–Si angle 106.9°; Figure 8). There is no indication of the pres-

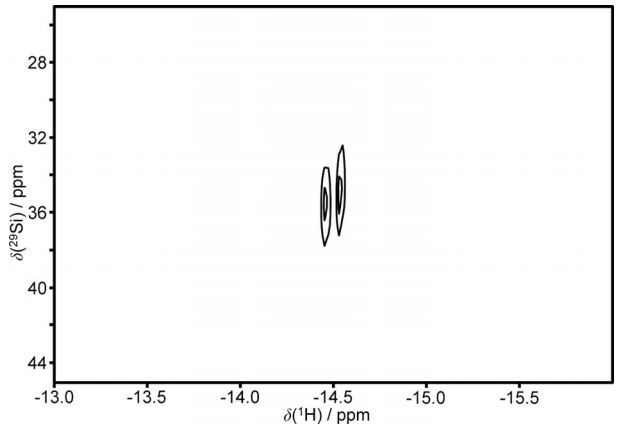

Figure 7. Part of the $^{1}H,^{29}Si$ HMBC NMR spectrum showing the resonance signal assigned to [Rh{κ²-(*N*,*N*)-(C_6F_5)*N*C(Me)-CHC(Me)*N*(C_6F_5)}($H)_2$($SiMe_3)_2$] (**16**).

ence of a non-classical structure (i.e., an interaction between a silyl and a hydrido ligand).[37] Note that often bis(silyl) complexes show a mutual *cis* orientation of the SiR_3 ligands,[36,38] but *trans* arrangements are also known[31,35] {e.g., in *cis*,*trans*-[Rh{κ²-(*N*,*N*)-(2,6-MeC_6H_3)-*N*C(Me)CHC(Me)*N*(2,6-MeC_6H_3)}($H)_2$($SiEt_3)_2$]}.[11]

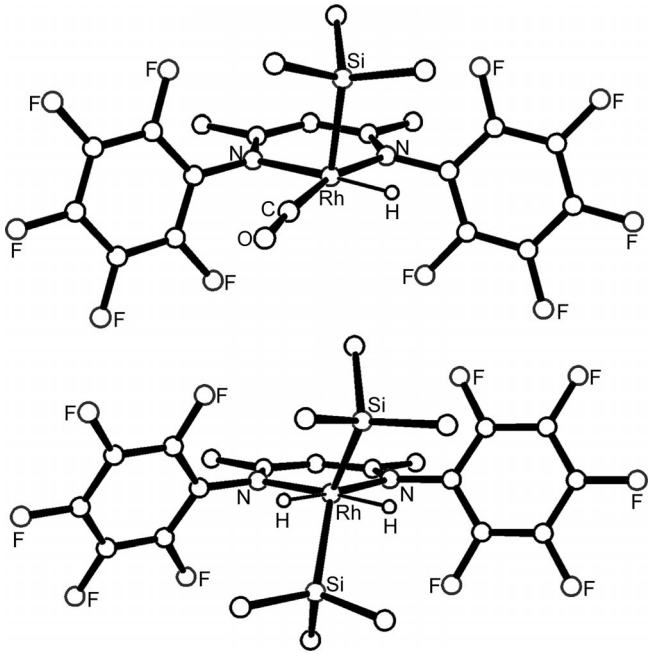

Figure 8. DFT/B3LYP-optimized geometries of [Rh{κ²-(*N*,*N*)-(C_6F_5)*N*C(Me)CHC(Me)*N*(C_6F_5)}(H)($SiMe_3$)(CO)] (**10a**) (top) and [Rh{κ²-(*N*,*N*)-(C_6F_5)*N*C(Me)CHC(Me)*N*(C_6F_5)}($H)_2$($SiMe_3)_2$] (**16**) (bottom). Ligand hydrogen atoms are omitted for clarity.

We did not observe a reaction of the silyl ligand with the β-diketiminato ligand in **10a** or **16**, as was described for *cis*,*trans*-[Rh{κ²-(*N*,*N*)-(2,6-MeC_6H_3)*N*C(Me)CHC(Me)*N*-(2,6-MeC_6H_3)}($H)_2$($SiEt_3)_2$].[11] Such a degradation reaction can be avoided by the use of the highly fluorinated β-diketimine **17**.

Conclusion

We have described the synthesis of new (β-ketiminato)- and (β-diketiminato)rhodium complexes that bear ligands with perfluorinated aryl groups. Stable carbonyl and isocyanide complexes with the β-diketiminato backbone were prepared. Treatment of [Rh{κ²-(*N*,*N*)-(C_6F_5)*N*C(Me)CHC-(Me)*N*(C_6F_5)}(CO)(NCMe)] (**7a**) with $HSiMe_3$ gave the (β-diketiminato)(hydrido)(silyl)rhodium complexes [Rh{κ²-(*N*,*N*)-(C_6F_5)*N*C(Me)CHC(Me)*N*(C_6F_5)}(H)($SiMe_3$)(CO)] (**10a**) and [Rh{κ²-(*N*,*N*)-(C_6F_5)*N*C(Me)CHC(Me)*N*-(C_6F_5)}($H)_2$($SiMe_3)_2$] (**16**). An Si–C coupling reaction between the silyl ligand and the β-diketiminato ligand in **10a** or **16** was not observed because of the presence of the fluorinated β-diketiminato ligand {(C_6F_5)NC(Me)CHC-(Me)N(C_6F_5)}.

Experimental Section

General Methods and Instrumentation: All experiments were performed with a Schlenk line under argon or an argon-filled glovebox with dioxygen levels below 10 ppm. All solvents were purified and dried by conventional methods and distilled under argon. Dipivaloyl methane, CN*t*Bu, 2,4-pentanedione, $HSiPh_3$, HSi(*i*Pr)$_3$, HSi-$(OMe)_3$, HSi$(OEt)_3$, $HSiEt_3$, Na_2CO_3, $MgSO_4$, $ONMe_3$, ^{13}CO, and HN*i*Pr_2 were obtained from Aldrich; *para*-toluenesulfonic acid, *n*BuLi, and 2,6-dimethylaniline were purchased from Acros Organics; KH, pentafluoroaniline, and $HSiMe_3$ were purchased from ABCR; CO was obtained from BASF. PEt_3,[39] (C_6F_5)NC(Me)-CHC(Me)NH(C_6F_5) (**17**),[15] (2,6-$Me_2C_6H_3$)NC(Me)CHC(Me)-NH(2,6-$Me_2C_6H_3$) (**21**),[40] [{Rh(μ-Cl)(cod)}$_2$],[41] [{Rh(μ-Cl)($C_2H_4)_2$}$_2$],[42] [{Rh(μ-Cl)(coe)$_2$}$_2$],[43] [{Rh(μ-Cl)$(CO)_2$}$_2$], and [{Rh(μ-Cl)($^{13}CO)_2$}$_2$][44] were prepared according to the literature. The NMR spectra were recorded with a Bruker DPX 300 or a Bruker AV III 300 spectrometer. Chemical shifts are reported in ppm. ^{1}H NMR spectroscopic chemical shifts were referenced to residual C_6D_5H at δ = 7.15 ppm or to residual [D_7]THF at δ = 3.58 ppm. $^{13}C\{^{1}H\}$ NMR spectroscopic chemical shifts were referenced to C_6D_6 at δ = 128.06 ppm or to [D_8]THF at δ = 67.21 ppm. The $^{31}P\{^{1}H\}$, ^{19}F, and ^{29}Si NMR spectra were referenced externally to H_3PO_3 at δ = 0.0 ppm, to C_6F_6 at δ = –162.9 ppm, and to $SiMe_4$ at δ = 0.0 ppm, respectively. Microanalyses were performed with a HEKAtech Euro EA Elemental Analyzer. Infrared spectra were recorded with a Bruker Vertex 70 spectrometer equipped with an ATR unit (diamond), and Raman spectra were recorded with a Bruker Vertex 70 with RAM II (Nd:YAG laser; 1064 nm). GC mass spectra were recorded with an Agilent 6890N gas chromatograph and an Agilent 5973 Network mass selective detector. The ESI mass spectra were recorded with an Esquire 3000 ion-trap mass spectrometer (Bruker), and LIFDI TOF mass spectra were recorded with a Micromass Q-ToF-2 mass spectrometer that was equipped with a LIFDI 700 ion source (Linden CMS).

(*t*Bu)(O)CCH_2C(*t*Bu)N(C_6F_5) (18): A solution of dipivaloyl methane (0.888 g, 4.8 mmol, 0.99 mL) in toluene (45 mL) was treated with pentafluoroaniline (1.830 g, 10.0 mmol) and *para*-toluenesulfonic acid (0.899 g, 4.7 mmol). The reaction mixture was heated under reflux conditions with a Dean–Stark apparatus for 48 h. Subsequently, most of the solvent was distilled off. After the solution had cooled to room temperature, volatile compounds were removed under vacuum. The obtained solid was dissolved in diethyl ether (25 mL) and water (25 mL). Sodium carbonate (1.098 g,

10.36 mmol) was added, and the solution was stirred at room temperature for 1.5 h. The aqueous layer was extracted two times each with Et_2O (15 mL), and the combined organic layers were dried with $MgSO_4$. The solvent was removed under vacuum. At –60 °C, the residue was washed with a small amount of hexane. The colorless solid was dissolved in hexane at room temperature, and the solution was stored at –30 °C. (*t*Bu)(O)CCH$_2$C(*t*Bu)N(C$_6$F$_5$) (**18**) was isolated as colorless crystalline solid. Yield: 1.111 g (4.2 mmol, 87%). $C_{17}H_{20}F_5NO$ (349.34): calcd. C 58.45, H 5.77, N 4.01; found C 59.10, H 6.05, N 4.53. IR (ATR): $\tilde{\nu}$ = 1710 (m, C=O), 1637 (m, C=N) cm^{-1}. ^{1}H NMR (300.1 MHz, C_6D_6, 25 °C): δ = 3.24 (s, 2 H, CH_2), 1.13 [s, 9 H, C(CH_3)$_3$], 0.60 [s, 9 H, C(CH_3)$_3$] ppm. ^{1}H NMR (300.1 MHz, THF/C_6D_6 capillary, 25 °C): δ = 2.79 (s, 2 H, CH_2), 1.28 [s, 9 H, C(CH_3)$_3$], 1.54 [s, 9 H, C(CH_3)$_3$] ppm. ^{13}C{^{1}H} NMR (75.5 MHz, C_6D_6, 25 °C): δ = 207.2 [s, *C*O or *C*N(C$_6$F$_5$)], 183.9 [s, *C*O or *C*N(C$_6$F$_5$)], 138.2 (dm, $^1J_{C,F}$ = 237.3 Hz, *C*F), 137.6 (dm, $^1J_{C,F}$ = 244.8 Hz, *C*F), 137.1 (dm, $^1J_{C,F}$ = 242.3 Hz, *C*F), 126.4 (m, C_{ipso}), 44.4 [s, *C*(CH$_3$)$_3$], 42.0 [s, *C*(CH$_3$)$_3$], 38.5 (s, *C*H$_2$), 27.4 (s, *C*H$_3$), 26.1 (s, *C*H$_3$) ppm. ^{19}F NMR (282.4 MHz, C_6D_6, 25 °C): δ = –152.5 (m, 2 F, *ortho*-C*F*), –164.3 (m, 2 F, *meta*-C*F*), –164.9 (m, 1 F, *para*-C*F*) ppm. ^{19}F NMR (282.4 MHz, THF/C_6D_6 capillary, 25 °C): δ = –153.3 (m, 2 F, *ortho*-C*F*), –165.9 (m, 2 F, *meta*-C*F*), –166.9 (m, 1 F, *para*-C*F*) ppm.

[K{(*t*Bu)(O)CCHC(*t*Bu)N(C$_6$F$_5$)}] (19): (*t*Bu)(O)CCH$_2$C(*t*Bu)N(C$_6$F$_5$) (**18**) (30 mg, 0.113 mmol) was dissolved in THF (1 mL) and treated with KH (8 mg, 0.190 mmol) at –20 °C. Gas evolution was observed, and the colorless solution turned yellow. The reaction mixture was stirred at room temperature for 30 min and analyzed by NMR spectroscopy. The NMR spectra indicate a quantitative reaction to yield **19**. ^{1}H NMR (300.1 MHz, THF/C_6D_6 capillary, 25 °C): δ = 5.46 (s, 1 H, C*H*), 1.54 [s, 9 H, C(CH_3)$_3$], 1.22 [s, 9 H, C(CH_3)$_3$] ppm. ^{19}F NMR (282.4 MHz, THF/C_6D_6 capillary, 25 °C): δ = –157.1 (m, 2 F), –171.5 (m, 2 F), –180.7 (m, 1 F) ppm.

[K{(C$_6$F$_5$)NC(Me)CHC(Me)N(C$_6$F$_5$)}] (20): (C$_6$F$_5$)NC(Me)CHC(Me)NH(C$_6$F$_5$) (**17**) (271 mg, 0.6 mmol) was dissolved in THF (8 mL). A suspension of KH (32 mg, 0.8 mmol) in THF (5 mL) was added dropwise at –30 °C through a polytetrafluoroethylene (PTFE) cannula. The solution was stirred, and gas evolution was observed. Within 2 h, the solution was allowed to reach room temperature. The clear yellow solution was analyzed by NMR spectroscopy. The NMR spectra indicate the formation of **20** in high yield. ^{1}H NMR (300.1 MHz, THF/C_6D_6 capillary, 25 °C): δ = 4.86 (s, 1 H, C*H*), 1.74 (s, 6 H, CH_3) ppm. ^{19}F NMR (282.4 MHz, THF/C_6D_6 capillary, 25 °C): δ = –156.0 (m, 4 F, *ortho*-C*F*), –168.3 (m, 4 F, *meta*-C*F*), –174.3 (m, 2 F, *para*-C*F*) ppm.

[Rh{κ^2-(*N*,*O*)-(*t*Bu)(*O*)CCHC(*t*Bu)*N*(C$_6$F$_5$)}(cod)] (1). (a) A solution of (*t*Bu)(O)CCH$_2$C(*t*Bu)N(C$_6$F$_5$) (**18**) (132 mg, 0.4 mmol) in THF (5 mL) was added dropwise at –40 °C through a PTFE cannula to a suspension of KH (24 mg, 0.6 mmol) in THF (5 mL). The reaction mixture was stirred at –40 °C for 15 min as well as at room temperature for 15 min. The yellow solution was then added dropwise at –40 °C to a solution of [{Rh(μ-Cl)(cod)}$_2$] (97 mg, 0.2 mmol). The mixture was allowed to reach room temperature slowly and afterwards stirred for 18 h. The color changed to reddish black. Volatile compounds were removed under vacuum. The residue was extracted two times each with toluene (4 mL). After removal of the solvent from the combined extracts under vacuum, the resulting solid was extracted two times each with hexane (6 mL). Concentration of the combined hexane phases under vacuum yielded [Rh{κ^2(*N*,*O*)-(*t*Bu)(*O*)CCHC(*t*Bu)*N*(C$_6$F$_5$)}(cod)] (**1**) as a pale yellow solid. Yield: 86 mg (0.2 mmol, 78%). **(b)** (*t*Bu)(O)CCH$_2$C(*t*Bu)N(C$_6$F$_5$) (**18**) (160 mg, 0.5 mmol) and lithium diisopropylamide (62 mg, 0.6 mmol) were treated with hexane (4 mL) and Et_2O (4 mL) at room temperature. After 30 min, the orange solution was transferred at –30 °C through a PTFE cannula to a solution of [{Rh(μ-Cl)(cod)}$_2$] (108 mg, 0.2 mmol) in Et_2O (5 mL). The mixture was stirred at –30 °C for 1.5 h. Subsequently, Et_2O (4 mL) and THF (5 mL) were added and stirred at room temperature for 3 h. The solution turned brownish yellow. The volatile compounds were removed under vacuum, and the residue was extracted two times each with toluene (5 mL). After removal of the solvent from the combined extracts under vacuum, the resulting solid was extracted two times each with hexane (6 mL). Concentration of the combined hexane phases under vacuum yielded [Rh{κ^2(*N*,*O*)-(*t*Bu)(*O*)CCHC(*t*Bu)*N*(C$_6$F$_5$)}(cod)] (**1**) as a pale yellow solid. Yield: 99 mg (0.2 mmol, 81%). $C_{25}H_{31}F_5NORh$ (559.42): calcd. C 53.68, H 5.59, N 2.50; found C 53.32, H 5.89, N 2.12. ^{1}H NMR (300.1 MHz, C_6D_6, 25 °C): δ = 5.76 (s, 1 H, C*H*), 4.57 (br. s, 2 H, cod-C*H*), 2.71 (br. s, 2 H, cod-C*H*), 2.12 (m, 4 H, cod-CH_2), 1.49 (m, 4 H, cod-CH_2), 1.13 [s, 9 H, C(CH_3)$_3$], 0.94 [s, 9 H, C(CH_3)$_3$] ppm. ^{13}C{^{1}H} NMR (75.5 MHz, C_6D_6, 25 °C): δ = 191.3 [s, *C*O or *C*N(C$_6$F$_5$)], 177.2 [s, *C*O or *C*N(C$_6$F$_5$)], 141.7 (dm, $^1J_{C,F}$ = 242.6 Hz, *C*F), 138.0 (dm, $^1J_{C,F}$ = 250.5 Hz, *C*F), 137.7 (dm, $^1J_{C,F}$ = 251.5 Hz, *C*F), 128.3 (m, C_{ipso}), 93.0 [d, $J_{Rh,C}$ = 1.9 Hz, (*t*Bu)(O)-C*C*HC(*t*Bu)N(C$_6$F$_5$)], 82.0 (d, $J_{Rh,C}$ = 12.9 Hz, cod-*C*H), 77.1 (d, $J_{Rh,C}$ = 14.3 Hz, cod-*C*H), 42.6 [s, *C*(CH$_3$)$_3$], 40.8 [s, *C*(CH$_3$)$_3$], 31.9 (s, cod-*C*H$_2$), 31.7 [s, C(*C*H$_3$)$_3$], 29.1 (s, cod-*C*H$_2$), 29.0 [s, C-(*C*H$_3$)$_3$] ppm. ^{19}F NMR (282.4 MHz, C_6D_6, 25 °C): δ = –144.6 (m, 2 F, *ortho*-C*F*), –161.3 (t, $^3J_{F,F}$ = 22.4 Hz, 1 F, *para*-C*F*), –164.0 (m, 2 F, *meta*-C*F*) ppm.

[Rh{κ^2-(*N*,*N*)-(C$_6$F$_5$)*N*C(Me)CHC(Me)*N*(C$_6$F$_5$)}(cod)] (2): (C$_6$F$_5$)NC(Me)CHC(Me)NH(C$_6$F$_5$) (**17**) (225 mg, 0.52 mmol) and KH (29.4 mg, 0.73 mmol) were treated with THF (7 mL) at –40 °C. The reaction mixture was allowed to reach room temperature and was stirred for 2.5 h. The solution was transferred at –70 °C through a PTFE cannula to a suspension of [{Rh(μ-Cl)(cod)}$_2$] (120 mg, 0.24 mmol) in THF (8 mL). The solution was allowed to reach room temperature and was stirred overnight. The volatile compounds were then removed under vacuum. The residue was extracted three times each with toluene (6 mL). The solvent was removed under vacuum from the combined extracts. The resulting solid was washed three times each with hexane (4 mL) at –40 °C. The residue was dried under vacuum to yield [Rh{κ^2(*N*,*N*)-(C$_6$F$_5$)-*N*C(Me)CHC(Me)*N*(C$_6$F$_5$)}(cod)] (**2**) as a beige solid. Yield: 139.8 mg (0.22 mmol, 91%). $C_{25}H_{19}F_{10}N_2Rh$ (640.32): calcd. C 46.89, H 2.99, N 4.37; found C 47.20, H 2.77, N 3.99. ^{1}H NMR (300.1 MHz, C_6D_6, 25 °C): δ = 4.98 (s, 1 H, C*H*), 3.31 (br. s, 4 H, cod-C*H*), 1.96 (m, 4 H, cod-C*H*H), 1.38 (s, 6 H, CH_3), 1.32 (m, 4 H, cod-CH*H*) ppm. ^{13}C{^{1}H} NMR (75.5 MHz, C_6D_6, 25 °C): δ = 163.2 [s, *C*N(C$_6$F$_5$)], 142.0 (dm, $^1J_{C,F}$ = 243.0 Hz, *C*F), 138.0 (dm, $^1J_{C,F}$ = 254.2 Hz, *C*F), 138.6 (dm, $^1J_{C,F}$ = 249.2 Hz, *C*F), 126.8 (m, C_{ipso}), 100.8 [d, $J_{Rh,C}$ = 1.5 Hz, C(Me)*C*HC(Me)], 79.1 (d, J = 12.7 Hz, cod-*C*H), 30.4 (s, cod*C*H$_2$), 24.9 (s, *C*H$_3$) ppm. ^{19}F NMR (282.4 MHz, C_6D_6, 25 °C): δ = –147.8 (m, 4 F, *ortho*-C*F*), –159.0 (t, $^3J_{F,F}$ = 22.4 Hz, 2 F, *para*-C*F*), –162.9 (m, 4 F, *meta*-C*F*) ppm.

[Rh{κ^2-(*N*,*N*)-(C$_6$F$_5$)*N*C(Me)CHC(Me)*N*(C$_6$F$_5$)}(C$_2$H$_4$)$_2$] (3): THF (8 mL) was added to (C$_6$F$_5$)NC(Me)CHC(Me)NH(C$_6$F$_5$) (**17**) (165 mg, 0.39 mmol) and KH (22 mg, 0.54 mmol) at –65 °C. The reaction mixture was stirred at –60 °C for 15 min and afterwards at room temperature for 3 h. The pale yellow solution was transferred dropwise through a PTFE cannula at –70 °C to a solution of [{Rh(μ-Cl)(C$_2$H$_4$)$_2$}$_2$] (68 mg, 0.18 mmol) in THF (7.5 mL). The reaction mixture was stirred at –60 °C for 30 min and at room temperature for 18 h while the color turned dark red. The volatile compounds were then removed under vacuum. The residue was ex-

tracted with toluene (7 mL). After removal of the solvent from the extract under vacuum, the solid was washed three times each with pentane (3 mL) at –50 °C. The residue was dried under vacuum to yield [Rh{κ²(*N*,*N*)-(C$_6$F$_5$)*N*C(Me)CHC(Me)*N*(C$_6$F$_5$)}(C$_2$H$_4$)$_2$] (**3**) as a yellow solid. Yield: 152 mg (0.27 mmol, 74%). LIFDI TOF MS: calcd. (%) for $C_{21}H_{15}F_{10}N_2Rh^+$ [M]$^+$ 588.2; found 588.2 (100); calcd. (%) for $C_{19}H_{11}F_{10}N_2Rh^+$ [M – (C$_2$H$_4$)]$^+$ 560.2; found 560.2 (65). ^{1}H NMR (300.1 MHz, C$_6$D$_6$, 25 °C): δ = 4.96 (s, 1 H, C*H*), 2.45 (m, 4 H, CH*H*), 1.73 (m, 4 H, C*H*H), 1.36 (s, 6 H, C*H*$_3$) ppm. ^{13}C{^{1}H} NMR (75.5 MHz, C$_6$D$_6$, 25 °C): δ = 163.0 [s, *C*N(C$_6$F$_5$)], 142.1 (dm, $^1J_{C,F}$ = 244.3 Hz, *C*F), 138.9 (dm, $^1J_{C,F}$ = 241.1 Hz, *C*F), 138.0 (dm, $^1J_{C,F}$ = 251.0 Hz, *C*F), 125.7 (m, *C*$_{ipso}$), 100.7 [d, $J_{Rh,C}$ = 1.3 Hz, NC(Me)*C*HC(Me)N], 61.5 (d, $J_{Rh,C}$ = 12.4 Hz, *C*H$_2$), 25.0 (s, *C*H$_3$) ppm. ^{19}F NMR (282.4 MHz, C$_6$D$_6$, 25 °C): δ = –147.2 (m, 4 F, *ortho*-C*F*), –158.2 (t, $^3J_{F,F}$ = 22.2 Hz, 2 F, *para*-C*F*), –162.9 (m, 4 F, *meta*-C*F*) ppm.

[Rh{κ²-(*N*,*N*)-(C$_6$F$_5$)*N*C(Me)CHC(Me)*N*(C$_6$F$_5$)}(CN*t*Bu)$_2$] (4): At –40 °C (C$_6$F$_5$)NC(Me)CHC(Me)NH(C$_6$F$_5$) (**17**) (258 mg, 0.60 mmol) and KH (34 mg, 0.84 mmol) were treated with THF (9 mL). The mixture was allowed to reach room temperature slowly and stirred at room temperature for 4 h. The solution was transferred at –70 °C through a PTFE cannula to a suspension of [{Rh(μ-Cl)(coe)$_2$}$_2$] (226 mg, 0.30 mmol) in THF (8 mL). The solution was allowed to reach room temperature and stirred overnight. A solution of CN*t*Bu (100 mg, 137 μL, 1.20 mmol) in THF (5 mL) was slowly added dropwise to the dark red reaction mixture. The solution was stirred at room temperature for 1 h. The volatile compounds were then removed under vacuum. The residue was extracted with toluene (10 mL). After evaporation of the solvent, the residue was extracted six times each with hexane (5 mL). The volume of the combined hexane phases was reduced under vacuum to approximately 10 mL. The solution was stored at –30 °C, which led to the precipitation of a pale yellow solid. After 48 h, the solid was filtered off at –30 °C. The residue was dried under vacuum to yield [Rh{κ²-(*N*,*N*)-(C$_6$F$_5$)*N*C(Me)CHC(Me)*N*(C$_6$F$_5$)}(CN*t*Bu)$_2$] (**4**) as a pale yellow powder. Yield: 172 mg (0.25 mmol, 82%). $C_{27}H_{25}F_{10}N_4Rh$ (698.40): calcd. C 46.43, H 3.61, N 8.02; found C 46.61, H 3.95, N 7.66. IR (ATR): $\tilde{\nu}$ = 2137 (m, CN*t*Bu), 2094 (m, CN*t*Bu), 2064 (m, CN*t*Bu) cm^{-1}. ^{1}H NMR (300.1 MHz, C$_6$D$_6$, 25 °C): δ = 5.04 (s, 1 H, C*H*), 1.51 (s, 6 H, C*H*$_3$), 0.73 [s, 18 H, C(C*H*$_3$)$_3$] ppm. ^{13}C{^{1}H} NMR (75.5 MHz, C$_6$D$_6$, 25 °C): δ = 161.6 [s, *C*N(C$_6$F$_5$)], 147.8 [d, $^1J_{Rh,C}$ = 65.1 Hz, Rh*C*NC(CH$_3$)$_3$], 142.1 (dm, $^1J_{C,F}$ = 244.9 Hz, *C*F), 139.3 (dm, $^1J_{C,F}$ = 250.3 Hz, *C*F), 138.1 (dm, $^1J_{C,F}$ = 250.3 Hz, *C*F), 133.8 (m, *C*$_{ipso}$), 100.3 [d, $J_{Rh,C}$ = 2.0 Hz, NC(Me)*C*HC(Me)N], 55.8 [s, CN*C*(CH$_3$)$_3$], 30.4 [s, CNC(*C*H$_3$)$_3$], 23.2 (s, *C*H$_3$) ppm. ^{19}F NMR (282.4 MHz, C$_6$D$_6$, 25 °C): δ = –147.9 (m, 4 F, *ortho*-C*F*), –164.7 (t, $^3J_{F,F}$ = 22.0 Hz, 2 F, *para*-C*F*), –165.5 (m, 4 F, *meta*-C*F*) ppm.

[Rh{κ²(*N*,*N*)-(2,6-Me$_2$C$_6$H$_3$)*N*C(Me)CHC(Me)*N*(2,6-Me$_2$C$_6$H$_3$)}-(CN*t*Bu)$_2$] (5): (2,6-Me$_2$C$_6$H$_3$)NC(Me)CHC(Me)NH(2,6-Me$_2$C$_6$H$_3$) (**21**) (129 mg, 0.4 mmol) was dissolved in THF (9 mL). At –40 °C *n*BuLi (1.6 mol L^{-1} solution in hexane, 0.33 mL, 0.5 mmol *n*BuLi) was added carefully. The mixture was stirred at –30 °C for 3 h, and the colorless solution turned yellow. The reaction solution was transferred slowly at –50 °C through a PTFE cannula to a suspension of [{Rh(μ-Cl)(coe)$_2$}$_2$] (152 mg, 0.2 mmol) in THF (9 mL). The solution was stirred for 3 h and allowed to reach room temperature. The color of the solution changed from ruby to a reddish black. A solution of CN*t*Bu (70 mg, 97 μL, 0.8 mmol) in THF (7.5 mL) was then added dropwise at room temperature. The solution was stirred at room temperature for 18 h. The volatile compounds were removed under vacuum. The residue was extracted with toluene (7 mL), and the solvent was removed from the extract under vacuum. The pale brown solid was washed at –30 °C three times each with hexane (4 mL). The beige solid was dissolved in toluene (7 mL) and layered with hexane (2 mL). This solution was stored at –30 °C. After 5 d, the solution was filtered at –30 °C. The residue was dried under vacuum to yield [Rh{κ²(*N*,*N*)-(2,6-Me$_2$C$_6$H$_3$)*N*C(Me)CHC(Me)*N*(2,6-Me$_2$C$_6$H$_3$)}-(CN*t*Bu)$_2$] (**5**) as a beige microcrystalline solid. Yield: 180 mg (0.3 mmol, 74%). $C_{31}H_{43}N_4Rh$ (574.61): calcd. C 64.80, H 7.54, N 9.75; found C 64.28, H 7.46, N 9.48. IR (ATR): $\tilde{\nu}$ = 2140 (vs, CN*t*Bu), 2103 (m, CN*t*Bu), 2068 (s, CN*t*Bu) cm^{-1}. ^{1}H NMR (300.1 MHz, C$_6$D$_6$, 25 °C): δ = 7.05 (br. d, $^3J_{H,H}$ = 7.4 Hz, 4 H, *meta*-Ar*H*), 6.91 (br. t, $^3J_{H,H}$ = 7.4 Hz, 2 H, *para*-Ar*H*), 5.13 [s, 1 H, NC(Me)C*H*C(Me)N], 2.56 (s, 12 H, ArC*H*$_3$), 1.62 (s, 6 H, C*H*$_3$), 0.81 [s, 18 H, C(C*H*$_3$)$_3$] ppm. ^{13}C{^{1}H} NMR (75.5 MHz, C$_6$D$_6$, 25 °C): δ = 158.1 (s, *C*=N or *C*$_{ipso}$), 157.3 (s, *C*=N or *C*$_{ipso}$), 150.5 [d, $^1J_{Rh,C}$ = 63.0 Hz, Rh*C*NC(CH$_3$)$_3$], 131.9 (s, C$_{Ar}$CH$_3$), 127.8 (s, *meta*-C$_{Ar}$H), 123.4 (s, *para*-C$_{Ar}$H), 97.5 [d, $J_{Rh,C}$ = 2.4 Hz, NC(Me)*C*HC(Me)N], 54.8 [s, CN*C*(CH$_3$)$_3$], 30.4 [s, CNC(*C*H$_3$)$_3$], 22.7 (s, *C*H$_3$), 19.7 (s, C$_{Ar}$*C*H$_3$) ppm.

[Rh{κ²-(*N*,*N*)-(C$_6$F$_5$)*N*C(Me)CHC(Me)*N*(C$_6$F$_5$)}(CO)$_2$] (6a): (C$_6$F$_5$)-NC(Me)CHC(Me)NH(C$_6$F$_5$) (**17**) (226.4 mg, 0.53 mmol) and KH (26.4 mg, 0.66 mmol) were treated with THF (8 mL) at –30 °C. The mixture was stirred at room temperature for 2 h. The yellow solution was added dropwise through a PTFE cannula to a yellow suspension of [{Rh(μ-Cl)(CO)$_2$}$_2$] (93.0 mg, 0.24 mmol) in THF (10 mL) at –70 °C. The solution was allowed to reach room temperature and stirred at room temperature for 15 h. The color of the solution turned to reddish black. The volatile compounds were then removed under vacuum. The residue was extracted two times each with toluene (10 mL), and afterwards the solvent was evaporated from the combined extracts. The pale yellow solid was washed at –90 °C five times each with pentane (5 mL). The residue was dried under vacuum to yield [Rh{κ²(*N*,*N*)-(C$_6$F$_5$)*N*C(Me)CHC(Me)*N*(C$_6$F$_5$)}(CO)$_2$] (**6a**) as a beige solid. The solvent was removed from the combined pentane fractions. The resulting residue was dissolved in CH_2Cl_2 and stored at –30 °C. After 3 d, the solution was filtered at –30 °C by using a cannula. The residue was dried under vacuum to yield 2,3,4,5,6-pentafluoro-*N*-[(*Z*)-6,7,8,9-tetrafluoro-2-methyl-1*H*-benzo[*b*]azepine-4(5*H*)-ylidene]benzeneamine (**22**) as a colorless crystalline solid (see the Supporting Information). Yield: **22**: 22 mg (0.05 mmol, 10%); **6a**: 121 mg (0.21 mmol, 86%). Spectroscopic data for **6a**: $C_{19}H_7F_{10}N_2O_2Rh$ (588.16): calcd. C 38.80, H 1.20, N 4.76; found C 39.26, H 1.16, N 4.96. Accurate ESI-MS$^+$: calcd. for $C_{19}H_8F_{10}N_2O_2Rh^+$ [M + H]$^+$: 588.9473; found 588.9476. Accurate ESI-MS$^-$: calcd. for $C_{19}H_6F_{10}N_2O_2Rh$ [MH]$^-$: 586.9327; found 586.9330; calcd. for $C_{19}H_7ClF_{10}N_2O_2Rh$ [M + Cl]$^-$: 622.9097; found 622.9097. GC–MS: t_R = 23.0 min; *m*/*z* = 28, 103, 181, 208, 249, 296, 532 [M – 2 CO]$^+$, 560 [M – CO]$^+$, 588 [M]$^+$. IR (ATR): $\tilde{\nu}$ = 2070 (s, CO), 2020 (s, CO) cm^{-1}. ^{1}H NMR (300.1 MHz, C$_6$D$_6$, 25 °C): δ = 4.90 (s, 1 H, C*H*), 1.34 (s, 6 H, C*H*$_3$) ppm. ^{1}H NMR (300.1 MHz, [D$_8$]THF, 25 °C): δ = 5.55 (s, 1 H, C*H*), 1.94 (s, 6 H, C*H*$_3$) ppm. ^{1}H NMR (300.1 MHz, 1,2-C$_6$H$_4$F$_2$/C$_6$D$_6$ capillary, 25 °C): δ = 5.15 (s, 1 H, C*H*), 1.68 (s, 6 H, C*H*$_3$) ppm. ^{19}F NMR (282.4 MHz, C$_6$D$_6$, 25 °C): δ = –148.2 (m, 4 F, *ortho*-C*F*), –158.6 (t, $^3J_{F,F}$ = 22.3 Hz, 2 F, *para*-C*F*), –162.6 (m, 4 F, *meta*-C*F*) ppm. ^{19}F NMR (282.4 MHz, [D$_8$]-THF, 25 °C): δ = –149.4 (m, 4 F, *ortho*-C*F*), –161.3 (t, $^3J_{F,F}$ = 22.3 Hz, 2 F, *para*-C*F*), –164.6 (m, 4 F, *meta*-C*F*) ppm. ^{19}F NMR (282.4 MHz, 1,2-C$_6$H$_4$F$_2$/C$_6$D$_6$ capillary, 25 °C): δ = –149.2 (m, 4 F, *ortho*-C*F*), –160.6 (t, $^3J_{F,F}$ = 22.3 Hz, 2 F, *para*-C*F*), –164.2 (m, 4 F, *meta*-C*F*) ppm. Spectroscopic data for **22**: $C_{17}H_7F_9N_2$ (410.24): calcd. C 49.77, H 1.72, N 6.83; found C 50.18, H 1.49, N 7.15. GC–MS: t_R = 20.3 min; *m*/*z* = 28, 84, 216, 391 [M – F]$^+$, 410

$[M]^+$. IR (ATR): $\tilde{\nu}$ = 3425 (w, NH), 1623 (w, CN) cm^{-1}. ^1H NMR (300.1 MHz, C_6D_6, 25 °C): δ = 5.26 (br. s, 1 H, N*H*), 4.80 (s, 1 H, C*H*), 3.59 (s, 2 H, CH_2), 1.06 (s, 3 H, CH_3) ppm. ^{19}F NMR (282.4 MHz, C_6D_6, 25 °C): δ = –144.48 (m, 1 F), –153.27 (m, 2 F), –153.77 (m, 1 F), –157.54 (m, 1 F), –158.77 (m, 1 F), –161.57 (m, 1 F), –164.21 (m, 2 F) ppm.

[Rh{κ²-(*N*,*N*)-(C_6F_5)*N*C(Me)CHC(Me)*N*(C_6F_5)}(^{13}CO)$_2$] (6b): (C_6F_5)NC(Me)CHC(Me)NH(C_6F_5) (**17**) (362 mg, 0.84 mmol) and KH (41 mg, 1.03 mmol) were slowly treated with THF (10 mL) at –30 °C. The mixture was allowed to reach room temperature and stirred at room temperature for 5 h. The yellow solution was transferred at –70 °C with a PTFE cannula to a yellow suspension of [{Rh(μ-Cl)(^{13}CO)$_2$}$_2$] (147 mg, 0.37 mmol) in THF (10 mL). The solution was stirred at room temperature for 15 h while the color turned reddish brown. The volatile compounds were then removed under vacuum. The residue was extracted two times each with toluene (10 mL), and the solvent was removed under vacuum from the combined extracts. The pale yellow solid was washed at –70 °C five times each with hexane (7 mL). Evaporation of the solvent yielded [Rh{κ²(*N*,*N*)-(C_6F_5)*N*C(Me)CHC(Me)*N*(C_6F_5)}(^{13}CO)$_2$] (**6b**) as a beige solid. Yield: 408 mg (0.69 mmol, 93%). LIFDI TOF MS: calcd. (%) for $C_{17}{}^{13}C_2H_7F_{10}N_2O_2Rh^+$ $[M]^+$ 590.2; found 590.2 (100). IR (ATR): $\tilde{\nu}$ = 2022 (s, ^{13}CO), 1975 (s, ^{13}CO) cm^{-1}. $^{13}C\{^1H\}$ NMR (75.5 MHz, C_6D_6, 25 °C): δ = 184.4 (d, $^1J_{Rh,C}$ = 66.6 Hz, *C*=O), 164.0 (s, *C*=N), 141.6 (dm, $^1J_{C,F}$ = 246.2 Hz, *C*F), 139.6 (dm, $^1J_{C,F}$ = 253.8 Hz, *C*F), 138.0 (dm, $^1J_{C,F}$ = 254.9 Hz, *C*F), 132.6 (m, C_{ipso}), 101.3 (d, $J_{Rh,H}$ = 2.3 Hz, *C*H), 22.6 (s, CH_3) ppm.

[Rh{κ²(*N*,*N*)-(C_6F_5)*N*C(Me)CHC(Me)*N*(C_6F_5)}(CO)(NMe$_3$)] (23): [Rh{κ²(*N*,*N*)-(C_6F_5)*N*C(Me)CHC(Me)*N*(C_6F_5)}(CO)$_2$] (**6a**) (49 mg, 0.1 mmol) was dissolved in 1,2-difluorobenzene (2 mL) and treated with $ONMe_3$ (5.7 mg, 0.1 mmol). After 6 h, the gaseous phase was analyzed. CO_2 could be identified with the help of GC–MS. The orange solution was examined by IR and NMR spectroscopy. [Rh{κ²(*N*,*N*)-(C_6F_5)*N*C(Me)CHC(Me)*N*(C_6F_5)}(CO)(NMe$_3$)] (**23**) was the only rhodium species that could be identified. IR (ATR, concentration of a 1,2-$C_6H_4F_2$ solution of **23**): $\tilde{\nu}$ = 1954 (m, CO) cm^{-1}. ^1H NMR (300.1 MHz, 1,2-$C_6H_4F_2$/C_6D_6 capillary, 25 °C): δ = 5.05 (s, 1 H, C*H*), 2.79 [br. s, 9 H, N(CH_3)$_3$] 1.64 (s, 3 H, CH_3), 1.61 (s, 3 H, CH_3) ppm. ^{19}F NMR (282.4 MHz, 1,2-$C_6H_4F_2$/C_6D_6 capillary, 25 °C): δ = –148.0 (m, 2 F, *ortho*-C*F*), –150.0 (m, 2 F, *ortho*-C*F*), –164.2 (t, $^3J_{F,F}$ = 20.5 Hz, 1 F, *para*-C*F*), –164.8 (t, $^3J_{F,F}$ = 21.4 Hz, 1 F, *para*-C*F*), –166.0 (m, 2 F, *meta*-C*F*), –167.8 (m, 2 F, *meta*-C*F*) ppm.

[Rh{κ²-(*N*,*N*)-(C_6F_5)*N*C(Me)CHC(Me)*N*(C_6F_5)}(CO)(NCMe)] (7a): In a Schlenk tube [Rh{κ²-(*N*,*N*)-(C_6F_5)*N*C(Me)CHC(Me)*N*(C_6F_5)}(CO)$_2$] (**6a**) (100 mg, 0.17 mmol) and $ONMe_3$ (15 mg, 0.20 mmol) were treated with acetonitrile (20 mL) and stirred at room temperature overnight. The gaseous phase was analyzed, and CO_2 could be identified with the help of GC–MS. The solvent was removed under vacuum, and the crude product was washed five times each with hexane (7 mL) at room temperature. The residue was dried under vacuum to yield [Rh{κ²-(*N*,*N*)-(C_6F_5)*N*C(Me)CHC(Me)*N*(C_6F_5)}(CO)(NCMe)] (**7a**) as a yellow solid. Yield: 99.7 mg (0.17 mmol, 98%). $C_{20}H_{10}F_{10}N_3ORh$ (601.20): calcd. C 39.96, H 1.68, N 6.99; found C 39.91, H 1.96, N 6.48. Accurate ESI-MS: calcd. for $C_{20}H_{11}F_{10}N_3ORh^+$ [M + H]$^+$ 601.9792; found 601.9788. IR (ATR): $\tilde{\nu}$ = 2283 (vw, NCMe), 1992 (s, CO) cm^{-1}. ^1H NMR (300.1 MHz, C_6D_6, 25 °C): δ = 5.03 (s, 1 H, C*H*), 1.51 (s, 3 H, CH_3), 1.44 (s, 3 H, CH_3), 0.03 (s, 3 H, NCCH_3) ppm. ^{19}F NMR (282.4 MHz, C_6D_6, 25 °C): δ = –146.9 (m, 2 F, *ortho*-C*F*), –148.5 (m, 2 F, *ortho*-C*F*), –160.8 (t, $^3J_{F,F}$ = 22.1 Hz, 1 F, *para*-C*F*), –162.3 (t, $^3J_{F,F}$ = 22.2 Hz, 1 F, *para*-C*F*), –163.6 (m, 2 F, *meta*-C*F*), –165.3 (m, 2 F, *meta*-C*F*) ppm.

[Rh{κ²-(*N*,*N*)-(C_6F_5)*N*C(Me)CHC(Me)*N*(C_6F_5)}(^{13}CO)(NCMe)] (7b): In a Schlenk tube, [Rh{κ²-(*N*,*N*)-(C_6F_5)*N*C(Me)CHC(Me)*N*(C_6F_5)}(^{13}CO)$_2$] (**6b**) (70 mg, 0.12 mmol) and $ONMe_3$ (11 mg, 0.142 mmol) were treated with acetonitrile (20 mL). The reaction mixture was stirred overnight. The gaseous as well as the liquid phase were analyzed. In the gas phase, $^{13}CO_2$ was identified with the help of GC–MS. A resonance signal in the $^{13}C\{^1H\}$ NMR spectrum of the reaction solution at δ = 124.8 ppm could be attributed to $^{13}CO_2$ (ref. C_6D_6 capillary).[32] The volatile compounds were removed under vacuum, and the crude product was washed five times each with hexane (7 mL) at room temperature. The residue was dried under vacuum to yield [Rh{κ²(*N*,*N*)-(C_6F_5)*N*C(Me)CHC(Me)*N*(C_6F_5)}(^{13}CO)(NCMe)] (**7b**) as a yellow solid. Yield: 66 mg (0.11 mmol, 92%). LIFDI TOF MS: calcd. (%) for $C_{19}{}^{13}CH_{10}F_{10}N_3ORh^+$ $[M]^+$ 602.2; found 602.2 (100). IR (ATR): $\tilde{\nu}$ = 2283 (vw, NCMe), 1946 (s, ^{13}CO) cm^{-1}. $^{13}C\{^1H\}$ NMR (75.5 MHz, C_6D_6, 25 °C): δ = 188.8 (d, $^1J_{Rh,C}$ = 71.5 Hz, Rh*C*O), 162.7 (s, *C*=N), 161.8 (s, *C*=N), 145–125 (m, C_{Ar}), 124.5 (s, N*C*CH$_3$), 100.7 (d, *J* = 2.3 Hz, *C*H), 23.3 (s, CH_3), 22.9 (s, CH_3), 0.0 (s, NCCH_3) ppm.

[Rh{κ²-(*N*,*N*)-(C_6F_5)*N*C(Me)CHC(Me)*N*(C_6F_5)}(CO)(PEt$_3$)] (8a): A solution of [Rh{κ²-(*N*,*N*)-(C_6F_5)*N*C(Me)CHC(Me)*N*(C_6F_5)}(CO)(NCMe)] (**7a**) (22 mg, 0.04 mmol) in C_6D_6 (0.7 mL) was treated with PEt_3 (5.5 mg, 6.9 μL, 0.05 mmol) at room temperature. The orange-red solution was then examined by means of IR and NMR spectroscopy. [Rh{κ²-(*N*,*N*)-(C_6F_5)*N*C(Me)CHC(Me)*N*(C_6F_5)}(CO)(PEt_3)] (**8a**) was the sole rhodium species that could be identified. IR (ATR, concentration of a C_6D_6 solution of **8a**): $\tilde{\nu}$ = 1962 (s, CO) cm^{-1}. ^1H NMR (300.1 MHz, C_6D_6, 25 °C): δ = 4.76 (s, 1 H, C*H*), 1.47 (s, 3 H, CH_3), 1.45 (s, 3 H, CH_3), 1.44–1.38 [br. s, 6 H, P(CH_2CH_3)$_3$], 1.07–0.96 [br. s, 9 H, P(CH_2CH_3)$_3$] ppm. ^{19}F NMR (282.4 MHz, C_6D_6, 25 °C): δ = –149.2 (m, 2 F, *ortho*-C*F*), –155.0 (m, 2 F, *ortho*-C*F*), –165.2 (m, 2 F, *meta*-C*F*), –165.9 (m, 2 F, *meta*-C*F*), –167.1 (t, $^3J_{F,F}$ = 22.4 Hz, 1 F, *para*-C*F*), –168.9 (t, $^3J_{F,F}$ = 22.6 Hz, 1 F, *para*-C*F*) ppm. $^{31}P\{^1H\}$ NMR (121.5 MHz, C_6D_6, 70 °C): δ = 21.7 (d, $^1J_{Rh,P}$ = 125.8 Hz) ppm.

[Rh{κ²-(*N*,*N*)-(C_6F_5)*N*C(Me)CHC(Me)*N*(C_6F_5)}(^{13}CO)(PEt$_3$)] (8b): A solution of [Rh{κ²-(*N*,*N*)-(C_6F_5)*N*C(Me)CHC(Me)*N*(C_6F_5)}(^{13}CO)(NCMe)] (**7b**) (19 mg, 0.03 mmol) in C_6D_6 (0.6 mL) was treated with PEt_3 (5.0 mg, 6.2 μL, 0.04 mmol) at room temperature. The orange-red solution was then examined by means of IR and NMR spectroscopy. [Rh{κ²(*N*,*N*)-(C_6F_5)*N*C(Me)CHC(Me)*N*(C_6F_5)}(^{13}CO)(PEt_3)] (**8b**) was the sole rhodium species that could be identified. IR (ATR, concentration of a C_6D_6 solution of **8b**): $\tilde{\nu}$ = 1914 (s, ^{13}CO) cm^{-1}. $^{13}C\{^1H\}$ NMR (75.5 MHz, C_6D_6, 25 °C): δ = 191.9 (dd, $^1J_{Rh,C}$ = 67.6, $^2J_{P,C}$ = 17.5 Hz, Rh*C*O), 169.3 (s, *C*=N), 166.2 (s, *C*=N), 145–125 (m, C_{Ar}), 105.6 (br. s, *C*H), 20.7 (s, CH_3), 19.8 (s, CH_3), 17.0 [t, $^1J_{C,P}$ = 12.8 Hz, P(CH_2CH_3)$_3$], 8.3 [s, P(CH_2CH_3)$_3$] ppm. $^{31}P\{^1H\}$ NMR (121.5 MHz, C_6D_6, 70 °C): δ = 21.7 (dd, $^1J_{P,Rh}$ = 125.8 Hz, $^2J_{P,C}$ = 17.5 Hz) ppm.

[Rh{κ²-(*N*,*N*)-(C_6F_5)*N*C(Me)CHC(Me)*N*(C_6F_5)}(CO)(NH_3)] (9a): [Rh{κ²-(*N*,*N*)-(C_6F_5)*N*C(Me)CHC(Me)*N*(C_6F_5)}(CO)(NCMe)] (**7a**) (20 mg, 0.03 mmol) was dissolved in C_6D_6 (0.6 mL). For 5 min, NH_3 gas was bubbled through the reaction mixture with a cannula. The orange-red solution was then examined by means of IR and NMR spectroscopy. [Rh{κ²-(*N*,*N*)-(C_6F_5)*N*C(Me)CHC(Me)*N*(C_6F_5)}(CO)(NH_3)] (**9a**) was the sole rhodium species that could be identified. IR (ATR, concentration of a C_6D_6 solution of **9a**): $\tilde{\nu}$ = 1956 (m, CO) cm^{-1}. ^1H NMR (300.1 MHz, C_6D_6, 25 °C): δ = 5.02 (s, 1 H, C*H*), 1.44 (s, 3 H, CH_3), 1.42 (s, 3 H, CH_3), 0.62 (s, 3 H, NH_3) ppm. ^{19}F NMR (282.4 MHz, C_6D_6, 25 °C): δ = –147.2 (m, 2 F, *ortho*-C*F*), –149.2 (m, 2 F, *ortho*-C*F*), –159.8 (t,

$^3J_{F,F}$ = 22.3 Hz, 1 F, *para*-C*F*), –161.7 (t, $^3J_{F,F}$ = 22.1 Hz, 1 F, *para*-C*F*), –162.6 (m, 2 F, *meta*-C*F*), –164.1 (m, 2 F, *meta*-C*F*) ppm.

[Rh{κ²-(*N*,*N*)-(C_6F_5)*N*C(Me)CHC(Me)*N*(C_6F_5)}(^{13}CO)(NH_3)] (9b): [Rh{κ²-(*N*,*N*)-(C_6F_5)*N*C(Me)CHC(Me)*N*(C_6F_5)}(^{13}CO)(NCMe)] (**7b**) (21 mg, 0.03 mmol) was dissolved in C_6D_6 (0.6 mL). For 5 min, NH_3 gas was bubbled through the reaction mixture with a cannula. The orange-red solution was then examined by means of IR and NMR spectroscopy. [Rh{κ²-(*N*,*N*)-(C_6F_5)*N*C(Me)CHC(Me)*N*(C_6F_5)}(^{13}CO)(NH_3)] (**9b**) was the sole rhodium species that could be identified. IR (ATR, concentration of a C_6D_6 solution of **9b**): ṽ = 1910 (m, ^{13}CO) cm^{-1}. ^{13}C{^{1}H} NMR (75.5 MHz, C_6D_6, 25 °C): δ = 190.5 (d, $^1J_{Rh,C}$ = 74.6 Hz, Rh*C*O), 162.7 (s, *C*=N), 161.1 (s, *C*=N), 150–130 (m, C_{Ar}), 100.6 (d, $J_{Rh,C}$ = 2.5 Hz, *C*H), 23.7 (s, *C*H_3), 23.0 (s, *C*H_3) ppm.

Reaction of [Rh{κ²-(*N*,*N*)-(C_6F_5)*N*C(Me)CHC(Me)*N*(C_6F_5)}(CO)(NCMe)] (7a) with $HSiMe_3$: Trimethylsilane gas was bubbled through a solution of [Rh{κ²-(*N*,*N*)-(C_6F_5)*N*C(Me)CHC(Me)*N*(C_6F_5)}(CO)(NCMe)] (**7a**) (25 mg, 0.04 mmol) in C_6D_6 (1 mL) at room temperature for 5 min. The orange-red solution was then examined by means of IR and NMR spectroscopy. After 5 h, the resonance signals of **7a** could no longer be detected. The volatile compounds were cautiously removed under vacuum. The residue was dissolved in C_6D_6 (1 mL) and examined by means of IR and NMR spectroscopy. [Rh{κ²-(*N*,*N*)-(C_6F_5)*N*C(Me)CHC(Me)*N*(C_6F_5)}(H)($SiMe_3$)(CO)] (**10a**), [Rh{κ²-(*N*,*N*)-(C_6F_5)*N*C(Me)CHC(Me)*N*(C_6F_5)}$(H)_2(SiMe_3)_2$] (**16**), and (C_6F_5)NC(Me)CHC(Me)NH(C_6F_5) (**17**) could be identified. Integration of the ^{1}H and ^{19}F NMR spectroscopic signals showed a 12:1:1 ratio of **10a**/**16**/**17**. By increasing the reaction time to 8 h, the product ratio of **10a**/**16**/**17** changed to 5:2:3. IR (ATR, concentration of the solvent from a reaction mixture in C_6D_6): ṽ = 2072 (s, CO), 2025 (s, RhH), 2017 (s, RhH) cm^{-1}. Spectroscopic data for [Rh{κ²-(*N*,*N*)-(C_6F_5)*N*C(Me)CHC(Me)*N*(C_6F_5)}(H)($SiMe_3$)(CO)] (**10a**): ^{1}H NMR (300.1 MHz, C_6D_6, 25 °C): δ = 5.06 (s, 1 H, C*H*), 1.49 (s, 3 H, CH_3), 1.44 (s, 3 H, CH_3), 0.31 [s, 9 H, Si(CH_3)$_3$], –12.34 (d, $^1J_{Rh,H}$ = 22.2 Hz, 1 H, Rh*H*) ppm. ^{19}F NMR (282.4 MHz, C_6D_6, 25 °C): δ = –146.9 (m, 2 F, *ortho*-C*F*), –149.1 (m, 2 F, *ortho*-C*F*), –159.9 (m, 1 F, *para*-C*F*), –160.4 (m, 1 F, *para*-C*F*), –163.5 (m, 2 F, *meta*-C*F*), –163.7 (m, 2 F, *meta*-C*F*) ppm. A signal in the ^{29}Si NMR spectrum could not be detected. Spectroscopic data for {Rh[κ²-(*N*,*N*)-(C_6F_5)*N*C(Me)CHC(Me)*N*(C_6F_5)](H)$_2$($SiMe_3$)$_2$} (**16**): ^{1}H NMR (300.1 MHz, C_6D_6, 25 °C): δ = 5.05 (s, 1 H, C*H*), 1.48 (s, 6 H, CH_3), 0.29 [s, 18 H, Si(CH_3)$_3$], –14.50 (d, $^1J_{Rh,H}$ = 23.4 Hz, 2 H, Rh*H*) ppm. ^{19}F NMR (282.4 MHz, C_6D_6, 25 °C): δ = –147.6 (m, 4 F, *ortho*-C*F*), –161.6 (m, 2 F, *para*-C*F*), –163.4 (m, 4 F, *meta*-C*F*) ppm. ^{1}H,^{29}Si HMBC NMR (300.1/59.6 MHz, C_6D_6, 25 °C): δ = –14.50/35.5 [d, $^1J_{Rh,H}$ = 23.4 Hz, Rh(*H*)(*Si*Me_3)].

Reaction of [Rh{κ²-(*N*,*N*)-(C_6F_5)*N*C(Me)CHC(Me)*N*(C_6F_5)}(^{13}CO)(NCMe)] (7b) with $HSiMe_3$: Trimethylsilane gas was bubbled through a solution of [Rh{κ²-(*N*,*N*)-(C_6F_5)*N*C(Me)CHC(Me)*N*(C_6F_5)}(^{13}CO)(NCMe)] (**7b**) (25 mg, 0.04 mmol) in C_6D_6 (1 mL) at room temperature for 5 min. The orange-red solution was then examined by means of IR and NMR spectroscopy. After 5 h, the resonance signals of **7b** could no longer be detected. In the ^{13}C{^{1}H} NMR spectrum, the resonance signal at δ = 181.5 ppm could be assigned to ^{13}CO.[33] The volatile compounds were cautiously removed under vacuum. The residue was dissolved in C_6D_6 (1 mL) and examined by means of IR and NMR spectroscopy. [Rh{κ²-(*N*,*N*)-(C_6F_5)*N*C(Me)CHC(Me)*N*(C_6F_5)}(H)($SiMe_3$)(^{13}CO)] (**10b**) and [Rh{κ²-(*N*,*N*)-(C_6F_5)*N*C(Me)CHC(Me)*N*(C_6F_5)}$(H)_2(SiMe_3)_2$] (**16**) could be identified. IR (ATR, concentration of a C_6D_6 reaction mixture): ṽ = 2022 (s, ^{13}CO), 2025 (s, RhH), 2017 (s, RhH) cm^{-1}. Spectroscopic data for [Rh{κ²-(*N*,*N*)-(C_6F_5)*N*C(Me)CHC(Me)*N*(C_6F_5)}(H)($SiMe_3$)(^{13}CO)] (**10b**): ^{1}H NMR (300.1 MHz, C_6D_6, 25 °C): δ = 5.06 (s, 1 H, C*H*), 1.49 (s, 3 H, CH_3), 1.44 (s, 3 H, CH_3), 0.31 [s, 9 H, Si(CH_3)$_3$], –12.34 (dd, $^1J_{Rh,H}$ = 22.2 Hz, $^2J_{C,H}$ = 9.5 Hz, 1 H, Rh*H*) ppm. ^{13}C{^{1}H} NMR (75.5 MHz, C_6D_6, 25 °C): δ = 188.2 (d, $^1J_{Rh,C}$ = 67.1 Hz, Rh*C*O) ppm.

Reaction of [Rh{κ²-(*N*,*N*)-(C_6F_5)*N*C(Me)CHC(Me)*N*(C_6F_5)}(CO)(NCMe)] (7a) with $HSiEt_3$: A solution of [Rh{κ²-(*N*,*N*)-(C_6F_5)*N*C(Me)CHC(Me)*N*(C_6F_5)}(CO)(NCMe)] (**7a**) (15 mg, 0.025 mmol) in C_6D_6 (0.6 mL) was treated with triethylsilane (2.8 mg, 3.8 μL, 0.025 mmol) at room temperature. The orange-red solution was then examined by means of IR and NMR spectroscopy. [Rh{κ²-(*N*,*N*)-(C_6F_5)*N*C(Me)CHC(Me)*N*(C_6F_5)}(CO)(NCMe)] (**7a**), (C_6F_5)NC(Me)CHC(Me)NH(C_6F_5) (**17**), and [Rh{κ²-(*N*,*N*)-(C_6F_5)*N*C(Me)CHC(Me)*N*(C_6F_5)}(H)($SiEt_3$)(CO)] (**11**) could be identified. After a reaction time of 8 h, integration of the ^{1}H and ^{19}F NMR spectroscopic signals showed a 6:2:1 ratio of **7a**/**11**/**17**. Spectroscopic data of [Rh{κ²-(*N*,*N*)-(C_6F_5)*N*C(Me)CHC(Me)*N*(C_6F_5)}(H)($SiMe_3$)(CO)] (**11**): IR (ATR, concentration of a C_6D_6 reaction mixture): ṽ = 2025 (w, sh), 2018 (w), 2004 (vw) cm^{-1}. ^{1}H NMR (300.1 MHz, C_6D_6, 25 °C): δ = 5.06 (s, 1 H, C*H*), 1.47 (s, 3 H, CH_3), 1.46 (s, 3 H, CH_3), 0.95 (t, $^3J_{H,H}$ = 7.9 Hz, 9 H, CH_2CH_3), 0.53 (m, 6 H, CH_2CH_3), –12.30 (d, $^1J_{Rh,H}$ = 22.0 Hz, 1 H, Rh*H*) ppm. ^{19}F NMR (282.4 MHz, C_6D_6, 25 °C): δ = –145.8 (m, 2 F, *ortho*-C*F*), –150.1 (m, 2 F, *ortho*-C*F*), –160.1 (t, $^3J_{F,F}$ = 22.3 Hz, 1 F, *para*-C*F*), –160.6 (t, $^3J_{F,F}$ = 22.1 Hz, 1 F, *para*-C*F*), –162.9 (m, 2 F, *meta*-C*F*), –163.5 (m, 2 F, *meta*-C*F*) ppm.

Reaction of [Rh{κ²-(*N*,*N*)-(C_6F_5)*N*C(Me)CHC(Me)*N*(C_6F_5)}(CO)(NCMe)] (7a) with HSi*i*Pr_3: Triisopropylsilane (5.3 mg, 6.9 μL, 0.03 mmol) was added at room temperature to a solution of [Rh{κ²-(*N*,*N*)-(C_6F_5)*N*C(Me)CHC(Me)*N*(C_6F_5)}(CO)(NCMe)] (**7a**) (20 mg, 0.03 mmol) in C_6D_6 (0.7 mL). The orange-red solution was examined by means of NMR spectroscopy. In addition to [Rh{κ²-(*N*,*N*)-(C_6F_5)*N*C(Me)CHC(Me)*N*(C_6F_5)}(CO)(NCMe)] (**7a**) and (C_6F_5)NC(Me)CHC(Me)NH(C_6F_5) (**17**), [Rh{κ²-(*N*,*N*)-(C_6F_5)*N*C(Me)CHC(Me)*N*(C_6F_5)}(H)(Si*i*Pr_3)(CO)] (**12**) could be identified. After a reaction time of 2 d, integration of the ^{1}H and ^{19}F NMR spectroscopic signals showed a 20:2:1 ratio of **7a**/**12**/**17**. Spectroscopic data for [Rh{κ²-(*N*,*N*)-(C_6F_5)*N*C(Me)CHC(Me)*N*(C_6F_5)}(H)(Si*i*Pr_3)(CO)] (**12**): ^{1}H NMR (300.1 MHz, C_6D_6, 25 °C): δ = 5.08 (s, 1 H, C*H*), 1.58 (s, 3 H, CH_3), 1.47 (s, 3 H, CH_3), 0.99 [m, 3 H, C*H*(CH_3)$_2$], 0.88 [d, $^3J_{H,H}$ = 7.4 Hz, 18 H, CH(CH_3)$_2$], –12.39 (d, $^1J_{Rh,H}$ = 21.5 Hz, 1 H, Rh*H*) ppm. ^{19}F NMR (282.4 MHz, C_6D_6, 25 °C): δ = –146.8 (m, 2 F, *ortho*-C*F*), –147.9 (m, 2 F, *ortho*-C*F*), –160.2 (m, 1 F, *para*-C*F*), –160.6 (m, 1 F, *para*-C*F*), –163.1 (m, 2 F, *meta*-C*F*), –163.5 (m, 2 F, *meta*-C*F*) ppm.

Reaction of [Rh{κ²-(*N*,*N*)-(C_6F_5)*N*C(Me)CHC(Me)*N*(C_6F_5)}(CO)(NCMe)] (7a) with $HSiPh_3$: In an NMR spectroscopy tube [Rh{κ²-(*N*,*N*)-(C_6F_5)*N*C(Me)CHC(Me)*N*(C_6F_5)}(CO)(NCMe)] (**7a**) (10 mg, 0.02 mmol) and triphenylsilane (4.3 mg, 0.02 mmol) were treated with C_6D_6 (0.6 mL) at room temperature. The orange-red solution was then examined by means of NMR spectroscopy. In addition to [Rh{κ²-(*N*,*N*)-(C_6F_5)*N*C(Me)CHC(Me)*N*(C_6F_5)}(CO)(NCMe)] (**7a**) and (C_6F_5)NC(Me)CHC(Me)NH(C_6F_5) (**17**), [Rh{κ²-(*N*,*N*)-(C_6F_5)*N*C(Me)CHC(Me)*N*(C_6F_5)}(H)($SiPh_3$)(CO)] (**13**) could be identified. After a reaction time of 2 d, integration of the ^{1}H and ^{19}F NMR spectroscopic signals showed a 7:1:1 ratio of **7a**/**13**/**17**. Spectroscopic data for [Rh{κ²-(*N*,*N*)-(C_6F_5)*N*C(Me)CHC(Me)*N*(C_6F_5)}(H)($SiPh_3$)(CO)] (**13**): ^{1}H NMR (300.1 MHz, C_6D_6, 25 °C): δ = 7.31 (m, 6 H, Ar*H*),

7.06 (m, 9 H, Ar*H*), 5.32 (s, 1 H, C*H*), 1.55 (s, 3 H, CH_3), 1.47 (s, 3 H, CH_3), –11.58 (d, $^1J_{Rh,H}$ = 19.9 Hz, 1 H, Rh*H*) ppm. ^{19}F NMR (282.4 MHz, C_6D_6, 25 °C): δ = –147.9 (m, 2 F, *ortho*-C*F*), –148.2 (m, 2 F, *ortho*-C*F*), –160.0 (m, 1 F, *para*-C*F*), –161.2 (m, 1 F, *para*-C*F*), –163.5 (m, 2 F, *meta*-C*F*), –163.7 (m, 2 F, *meta*-C*F*) ppm.

Reaction of [Rh{κ²-(*N*,*N*)-(C_6F_5)*N*C(Me)CHC(Me)*N*(C_6F_5)}(CO)(NCMe)] (7a) with HSi(OMe)₃: Trimethoxysilane (2.9 mg, 3.0 μL, 0.02 mmol) was added at room temperature to a solution of [Rh{κ²-(*N*,*N*)-(C_6F_5)*N*C(Me)CHC(Me)*N*(C_6F_5)}(CO)(NCMe)] (**7a**) (14 mg, 0.02 mmol) in C_6D_6 (1 mL). The orange-red solution was then examined by means of NMR spectroscopy. In addition to [Rh{κ²-(*N*,*N*)-(C_6F_5)*N*C(Me)CHC(Me)*N*(C_6F_5)}(CO)(NCMe)] (**7a**) and (C_6F_5)NC(Me)CHC(Me)NH(C_6F_5) (**17**), [Rh{κ²(*N*,*N*)-(C_6F_5)*N*C(Me)CHC(Me)*N*(C_6F_5)}(H){Si(OMe)₃}(CO)] (**14**) could be identified. After a reaction time of 18 h, integration of the ^{1}H and ^{19}F NMR spectroscopic signals showed a 10:1:3 ratio of **7a**/**14**/**17**. Spectroscopic data for [Rh{κ²(*N*,*N*)-(C_6F_5)*N*C(Me)CHC(Me)-*N*(C_6F_5)}(H){Si(OMe)₃}(CO)] (**14**): ^{1}H NMR (300.1 MHz, C_6D_6, 25 °C): δ = 4.93 (s, 1 H, C*H*), 3.51 (s, 9 H, OCH_3), 1.56 (s, 3 H, CH_3), 1.49 (s, 3 H, CH_3), –12.29 (d, $^1J_{Rh,H}$ = 23.5 Hz, 1 H, Rh*H*) ppm. ^{19}F NMR (282.4 MHz, C_6D_6, 25 °C): δ = –146.5 (m, 2 F, *ortho*-C*F*), –148.2 (m, 2 F, *ortho*-C*F*), –158.6 (m, 1 F, *para*-C*F*), –159.6 (m, 1 F, *para*-C*F*), –162.6 (m, 2 F, *meta*-C*F*), –163.9 (m, 2 F, *meta*-C*F*) ppm.

Reaction of [Rh{κ²-(*N*,*N*)-(C_6F_5)*N*C(Me)CHC(Me)*N*(C_6F_5)}(CO)(NCMe)] (7a) with HSi(OEt)₃: [Rh{κ²-(*N*,*N*)-(C_6F_5)*N*C(Me)-CHC(Me)*N*(C_6F_5)}(CO)(NCMe)] (**7a**) (24 mg, 0.04 mmol) was dissolved in C_6D_6 (1 mL). Triethoxysilane (6.6 mg, 7.4 μL, 0.04 mmol) was added dropwise at room temperature. The orange-red solution was then examined by means of NMR spectroscopy. In addition to [Rh{κ²-(*N*,*N*)-(C_6F_5)*N*C(Me)CHC(Me)*N*(C_6F_5)}(CO)(NCMe)] (**7a**) and (C_6F_5)NC(Me)CHC(Me)NH(C_6F_5) (**17**), [Rh{κ²-(*N*,*N*)-(C_6F_5)*N*C(Me)CHC(Me)*N*(C_6F_5)}(H){Si(OEt)₃}(CO)] (**15**) could be identified. After a reaction time of 18 h, integration of the ^{1}H and ^{19}F NMR spectroscopic signals showed an 8:3:1 ratio of **7a**/**15**/**17**. Spectroscopic data for [Rh{κ²-(*N*,*N*)-(C_6F_5)*N*C(Me)CHC(Me)-*N*(C_6F_5)}(H){Si(OEt)₃}(CO)] (**15**): ^{1}H NMR (300.1 MHz, C_6D_6, 25 °C): δ = 5.05 (s, 1 H, C*H*), 3.64 (q, $^3J_{H,H}$ = 7.0 Hz, 6 H, OCH_2CH₃), 1.55 (s, 3 H, CH_3), 1.49 (s, 3 H, CH_3), 1.06 (t, $^3J_{H,H}$ = 7.0 Hz, 9 H, OCH$_2$CH_3), –12.17 (d, $^1J_{Rh,H}$ = 23.4 Hz, 1 H, Rh*H*) ppm. ^{19}F NMR (282.4 MHz, C_6D_6, 25 °C): δ = –148.4 (m, 2 F, *ortho*-C*F*), –149.2 (m, 2 F, *ortho*-C*F*), –160.5 (m, 1 F, *para*-C*F*), –160.9 (m, 1 F, *para*-C*F*), –163.2 (m, 2 F, *meta*-C*F*), –163.4 (m, 2 F, *meta*-C*F*) ppm.

Density Functional Calculations: All calculations were performed by using the Gaussian 09 (Revision C01)[45] program package with the B3LYP functional. The carbon, fluorine, and hydrogen atoms (except the metal-bound hydrogen atoms) were described by using the cc-pVDZ basis set. For nitrogen, silicon, and the metal-bound hydrogen atoms, the cc-pVTZ basis set was applied. In the case of **4**, all atoms except rhodium were described by using the cc-pVDZ basis set. Rhodium was described by using relativistic effective core potentials (RECPs) with the associated cc-pVDZ-PP basis set.[46] The nature of the minimum structures was verified by the absence of imaginary frequencies by frequency mode analyses.

Structural Determination: Diffraction data of **18**, **1**, **2**, **4**, **5**, **6a**, and **7a** were collected with a STOE IPDS 2θ diffractometer with Mo-K_α radiation (λ = 0.71073 Å) at 100 K. Crystallographic data are given below. The structures were solved by direct methods (SHELXS-97)[47] (except for compound **7a**, which was solved by SIR-97[48]) and refined with full-matrix least-square methods on F^2 (SHELX-97, SHELXL-2013).[47] The hydrogen atoms were placed at calculated positions and refined by using a riding model. CCDC-986662 (**1**), -986663 (**2**), -986664 (**4**), -986665 (**5**), -986666 (**6a**), -986667 (**7a**), and -986668 (**18**) contain the supplementary crystallographic data for this paper. These data can be obtained free of charge from The Cambridge Crystallographic Data Centre via www.ccdc.cam.ac.uk/data_request/cif.

Compound 18: $C_{17}H_{20}F_5NO$, M_r = 349.34, crystal dimensions 0.40 × 0.24 × 0.16 mm; monoclinic; $P2_1/c$; a = 10.4069(8) Å, b = 14.9575(9) Å, c = 11.3092(10) Å, β = 104.553(6)°, Z = 4, V = 1703.9(2) Å^3, $\rho_{calcd.}$ = 1.362 g cm^{-3}; $2\theta_{max}$ = 53.00; 3466 reflections collected, 3466 were unique (R_{int} = 0.0737), μ(Mo-K_α) = 0.122 mm^{-1}. Final R_1, wR_2, GoF values on all data: 0.1103, 0.0960, 1.027; R_1, wR_2, GoF values for reflections with $I_o > 2\sigma(I_o)$: 0.0595, 0.0850, 1.029; residual electron density: +0.19/–0.22 e Å^{-3}.

Compound 1: $C_{25}H_{31}F_5NORh$, M_r = 559.42, crystal dimensions 0.24 × 0.18 × 0.12 mm; monoclinic; $P2_1/c$; a = 14.0849(6) Å, b = 14.3360(7) Å, c = 12.7259(6) Å, β = 112.899(3)°, Z = 4, V = 2367.12(19) Å^3, $\rho_{calcd.}$ = 1.570 g cm^{-3}; $2\theta_{max}$ = 59.18°; 45634 reflections collected, 6388 were unique (R_{int} = 0.049), μ(Mo-K_α) = 0.78 mm^{-1}. Final R_1, wR_2, GoF values on all data: 0.0398, 0.0820, 1.112; R_1, wR_2, GoF values for reflections with $I_o > 2\sigma(I_o)$: 0.0342, 0.0845, 1.081; residual electron density: +1.32/–0.95 e Å^{-3}.

Compound 2: $C_{25}H_{19}F_{10}N_2Rh$, M_r = 640.33, crystal dimensions 0.20 × 0.20 × 0.05 mm; triclinic; $P\bar{1}$; a = 9.5142(4) Å, b = 11.3735(5) Å, c = 11.8158(5) Å, α = 77.144(4)°, β = 87.940(3)°, γ = 69.599(4)°, Z = 2, V = 1166.82(9) Å^3, $\rho_{calcd.}$ = 1.823 g cm^{-3}; $2\theta_{max}$ = 50.02°; 11681 reflections collected, 4105 were unique (R_{int} = 0.0579), μ(Mo-K_α) = 0.830 mm^{-1}. Final R_1, wR_2, GoF values on all data: 0.0247, 0.0670, 1.039; R_1, wR_2, GoF values for $I_o > 2\sigma(I_o)$: 0.0269, 0.0618, 1.039; residual electron density: +0.57/–0.72 e Å^{-3}.

Compound 4: $C_{27}H_{25}F_{10}N_4Rh$, M_r = 698.42, crystal dimensions 0.30 × 0.15 × 0.15 mm; monoclinic; $P2_1/c$; a = 15.5977(5) Å, b = 9.2673(4) Å, c = 19.8974(6) Å, β = 92.326(2)°, Z = 4, V = 2873.77(18) Å^3, $\rho_{calcd.}$ = 1.614 g cm^{-3}; $2\theta_{max}$ = 58.00°; 50085 reflections collected, 7638 were unique (R_{int} = 0.0812), μ(Mo-K_α) = 0.683 mm^{-1}. Final R_1, wR_2, GoF values on all data: 0.0508, 0.0846, 1.051; R_1, wR_2, GoF values for reflections with $I_o > 2\sigma(I_o)$: 0.0387, 0.0800, 1.051; residual electron density: +0.62/–0.74 e Å^{-3}.

Compound 5: $C_{31}H_{43}N_4Rh$, M_r = 574.60, crystal dimensions 0.40 × 0.20 × 0.14 mm; monoclinic; $C2/c$; a = 19.5039(6) Å, b = 16.2291(3) Å, c = 19.2485(6) Å, β = 105.313(2)°, Z = 8, V = 5876.4(3) Å^3, $\rho_{calcd.}$ = 1.299 g cm^{-3}; $2\theta_{max}$ = 55°; 46122 reflections collected, 6740 were unique (R_{int} = 0.0717), μ(Mo-K_α) = 0.606 mm^{-1}. Final R_1, wR_2, GoF values on all data: 0.0390, 0.0532, 1.018; R_1, wR_2, GoF values for reflections with $I_o > 2\sigma(I_o)$: 0.0286, 0.0509, 1.018; residual electron density: +0.43/–0.53 e Å^{-3}.

Compound 6a: $C_{19}H_7F_{10}N_2O_2Rh$, M_r = 588.18, crystal dimensions 0.28 × 0.20 × 0.08 mm; monoclinic; $P2_1/n$; a = 13.2668(5) Å, b = 7.5056(2) Å, c = 20.1044(6) Å, β = 98.908(3)°, Z = 4, V = 1977.75(11) Å^3, $\rho_{calcd.}$ = 1.975 g cm^{-3}; $2\theta_{max}$ = 58.36°; 20687 reflections collected, 5327 were unique (R_{int} = 0.0286), μ(Mo-K_α) = 0.977 mm^{-1}. Final R_1, wR_2, GoF values on all data: 0.0374, 0.0858, 1.054; R_1, wR_2, GoF values for reflections with $I_o > 2\sigma(I_o)$: 0.0333, 0.0836, 1.054; residual electron density: +1.07/–1.08 e Å^{-3}.

Compound 7a: $C_{20}H_{10}F_{10}N_3ORh$, M_r = 601.22, crystal dimensions 0.24 × 0.15 × 0.04 mm; triclinic; $P\bar{1}$; a = 7.3288(5) Å, b = 11.7219(8) Å, c = 12.8497(8) Å, α = 91.815(5)°, β = 106.069(5)°, γ = 102.360(6)°, Z = 2, V = 1031.30(12) Å^3, $\rho_{calcd.}$ = 1.936 g cm^{-3}; $2\theta_{max}$ = 56.42°; 11047 reflections collected, 4955 were unique (R_{int} = 0.0587), μ(Mo-K_α) = 0.937 mm^{-1}. Final R_1, wR_2, GoF values on all data: 0.0580, 0.0748, 0.989; R_1, wR_2, GoF values for reflections

with $I_o > 2\sigma(I_o)$: 0.0395, 0.0704, 0.989; residual electron density: +0.529/–0.770 e Å^{-3}.

Supporting Information (see footnote on the first page of this article): Experimental IR data and synthesis of **22**. Details on the DFT calculations as well as Cartesian coordinates for all optimized structures.

Acknowledgments

We would like to acknowledge the Deutsche Forschungsgemeinschaft (DFG) for financial support. The Cluster of Excellence "Unifying Concepts in Catalysis" (UniCat) funded by the DFG is gratefully acknowledged. We are grateful to Annemarie Bittner, Johannes Kohlmann, and Hanna Baumgarth for experimental assistance.

[1] a) L. Bourget-Merle, M. F. Lappert, J. R. Severn, *Chem. Rev.* **2002**, *102*, 3031–3065; b) Y.-C. Tsai, *Coord. Chem. Rev.* **2012**, *256*, 722–758; c) S. Pillai Sarish, S. Nembenna, S. Nagendra, H. W. Roesky, *Acc. Chem. Res.* **2011**, *44*, 157–170; d) H. W. Roesky, S. Singh, V. Jancik, V. Chandrasekhar, *Acc. Chem. Res.* **2004**, *37*, 969–981; e) H. Zhu, J. Chai, V. Jancik, H. W. Roesky, W. A. Merrill, P. P. Power, *J. Am. Chem. Soc.* **2005**, *127*, 10170–10171; f) P. L. Holland, *Acc. Chem. Res.* **2008**, *41*, 905–914; g) D. J. Mindiola, *Angew. Chem. Int. Ed.* **2009**, *48*, 6198–6200; *Angew. Chem.* **2009**, *121*, 6314–6316; h) W. E. Piers, D. J. H. Emslie, *Coord. Chem. Rev.* **2002**, *233–234*, 131–155; i) S. Yao, M. Driess, *Acc. Chem. Res.* **2012**, *45*, 276–287; j) C. J. Cramer, W. B. Tolman, *Acc. Chem. Res.* **2007**, *40*, 601–608; k) L. Boisvert, K. I. Goldberg, *Acc. Chem. Res.* **2012**, *45*, 899–910.

[2] See for example: a) K. C. MacLeod, B. O. Patrick, K. M. Smith, *Inorg. Chem.* **2012**, *51*, 688–700; b) J. Vela, J. M. Smith, Y. Yu, N. A. Ketterer, C. J. Flaschenriem, R. J. Lachicotte, P. L. Holland, *J. Am. Chem. Soc.* **2005**, *127*, 7857–7870; c) T. R. Dugan, K. C. MacLeod, W. W. Brennessel, P. L. Holland, *Eur. J. Inorg. Chem.* DOI: 10.1002/ejic.201300187; d) S. Yao, E. Bill, C. Milsmann, K. Wieghardt, M. Driess, *Angew. Chem. Int. Ed.* **2008**, *47*, 7110–7113; *Angew. Chem.* **2008**, *120*, 7218–7221; e) A. Company, S. Yao, K. Ray, M. Driess, *Chem. Eur. J.* **2010**, *16*, 9669–9675; f) S. Yao, C. Herwig, Y. Xiong, A. Company, E. Bill, C. Limberg, M. Driess, *Angew. Chem. Int. Ed.* **2010**, *49*, 7054–7058; *Angew. Chem.* **2010**, *122*, 7208–7212; g) S. Yao, Y. Xiong, M. Vogt, H. Grützmacher, C. Herwig, C. Limberg, M. Driess, *Angew. Chem. Int. Ed.* **2009**, *48*, 8107–8110; *Angew. Chem.* **2009**, *121*, 8251–8251; h) G. Bai, P. Wei, A. K. Das, D. W. Stephan, *Dalton Trans.* **2006**, 1141–1146; i) B. Horn, S. Pfirrmann, C. Limberg, C. Herwig, B. Braun, S. Mebs, R. Metzinger, *Z. Anorg. Allg. Chem.* **2011**, *637*, 1169–1174; j) S. Wiese, J. L. McAfee, D. R. Pahls, C. L. McMullin, T. R. Cundari, T. H. Warren, *J. Am. Chem. Soc.* **2012**, *134*, 10114–10121; k) C. Köthe, R. Metzinger, C. Herwig, C. Limberg, *Inorg. Chem.* **2012**, *51*, 9740–9747; l) B. Horn, C. Limberg, C. Herwig, S. Mebs, *Angew. Chem. Int. Ed.* **2011**, *50*, 12621–12625; *Angew. Chem.* **2011**, *123*, 12829–12833; m) S. Pfirrmann, C. Limberg, C. Herwig, R. Stößer, B. Ziemer, *Angew. Chem. Int. Ed.* **2009**, *48*, 3357–3361; *Angew. Chem.* **2009**, *121*, 3407–3411; n) D. J. Mindiola, *Angew. Chem. Int. Ed.* **2009**, *48*, 6198–6200; *Angew. Chem.* **2009**, *121*, 6314–6316; o) S. Pfirrmann, C. Limberg, C. Herwig, C. Knispel, B. Braun, E. Bill, R. Stösser, *J. Am. Chem. Soc.* **2010**, *132*, 13684–13691; p) S. Pfirrmann, C. Limberg, E. Hoppe, *Z. Anorg. Allg. Chem.* **2009**, *635*, 312–316; q) B. Horn, C. Limberg, C. Herwig, M. Feist, S. Mebs, *Chem. Commun.* **2012**, *48*, 8243–8245; r) S. Pfirrmann, S. Yao, B. Ziemer, R. Stößer, M. Driess, C. Limberg, *Organometallics* **2009**, *28*, 6855–6860; s) S. Pfirrmann, C. Limberg, B. Ziemer, *Dalton Trans.* **2008**, 6689–6691; t) G. Bai, P. Wei, D. W. Stephan, *Organometallics* **2005**, *24*, 5901–5908; u) C. Koethe, R. Metzinger, C. Herwig, C. Limberg, *Inorg. Chem.* **2012**, *51*, 9740–9747; v) S. Yao, P. Hrobárik, F. Meier, R. Rudolph, E. Bill, E. Irran, M. Kaupp, M. Driess, *Chem. Eur. J.* **2013**, *19*, 1246–1253; w) S. Wiese, M. J. B. Aguila, E. Kogut, T. H. Warren, *Organometallics* **2013**, *32*, 2300–2308; x) R. Sarangi, N. Aboelella, K. Fujisawa, W. B. Tolman, B. Hedman, K. O. Hodgson, E. I. Solomon, *J. Am. Chem. Soc.* **2006**, *128*, 8286–8296; y) R. T. Gephart, C. L. McMullin, N. G. Sapiezynski, E. S. Jang, M. J. B. Aguila, T. R. Cundari, T. H. Warren, *J. Am. Chem. Soc.* **2012**, *134*, 17350–17353; z) R. T. Gephart III, D. L. Huang, M. J. B. Aguila, G. Schmidt, A. Shahu, T. H. Warren, *Angew. Chem. Int. Ed.* **2012**, *51*, 6488–6492; *Angew. Chem.* **2012**, *124*, 6594–6598.

[3] See for example: a) J. Chai, H. Zhu, A. C. Stückl, H. W. Roesky, J. Magull, A. Bencini, A. Caneschi, D. Gatteschi, *J. Am. Chem. Soc.* **2005**, *127*, 9201–9206; b) A. K. Gupta, W. B. Tolman, *Inorg. Chem.* **2012**, *51*, 1811–1888; c) D.-H. Lee, J.-Y. Jung, M.-J. Jin, *Chem. Commun.* **2010**, *46*, 9046–9048; d) V. T. Annibale, L. M. Lund, D. Song, *Chem. Commun.* **2010**, *46*, 8261–8263; e) M. L. Scheuermann, U. Fekl, W. Kaminsky, K. I. Goldberg, *Organometallics* **2010**, *29*, 4749–4751; f) U. Fekl, W. Kaminsky, K. I. Goldberg, *J. Am. Chem. Soc.* **2001**, *123*, 6423–6424; g) U. Fekl, W. Kaminsky, K. I. Goldberg, *J. Am. Chem. Soc.* **2003**, *125*, 15286–15287; h) W. H. Bernskoetter, E. Lobkovsky, P. J. Chirik, *Chem. Commun.* **2004**, 764–765; i) W. H. Bernskoetter, E. Lobkovsky, P. J. Chirik, *Organometallics* **2005**, *24*, 4367–4373; j) W. H. Bernskoetter, E. Lobkovsky, P. J. Chirik, *Organometallics* **2005**, *24*, 6250–6259.

[4] a) P. H. M. Budzelaar, N. N. P. Moonen, R. de Gelder, J. M. M. Smits, A. W. Gal, *Chem. Eur. J.* **2000**, *6*, 2740–2747; b) S. T. H. Willems, P. H. M. Budzelaar, N. N. P. Moonen, R. de Gelder, J. M. M. Smits, A. W. Gal, *Chem. Eur. J.* **2002**, *8*, 1310–1320.

[5] a) P. H. M. Budzelaar, N. N. P. Moonen, R. de Gelder, J. M. M. Smits, A. W. Gal, *Eur. J. Inorg. Chem.* **2000**, 753–769; b) P. H. M. Budzelaar, R. de Gelder, A. W. Gal, *Organometallics* **1998**, *17*, 4121–4123.

[6] S. J. Geier, D. W. Stephan, *Chem. Commun.* **2008**, 2779–2781.

[7] D. W. Shaffer, S. A. Ryken, R. A. Zarkesh, A. F. Heyduk, *Inorg. Chem.* **2011**, *50*, 13–21.

[8] D. W. Shaffer, S. A. Ryken, R. A. Zarkesh, A. F. Heyduk, *Inorg. Chem.* **2012**, *51*, 12122–12131.

[9] J. D. Masuda, D. W. Stephan, *Can. J. Chem.* **2005**, *83*, 324–327.

[10] S. J. Geier, D. W. Stephan, *Chem. Commun.* **2008**, 99–101.

[11] D. Zhu, D. J. Kozera, K. D. Enns, P. H. M. Budzelaar, *Angew. Chem. Int. Ed.* **2012**, *51*, 12211–12214; *Angew. Chem.* **2012**, *124*, 12377–12380.

[12] a) K. Spannhoff, G. Kehr, S. Kehr, R. Fröhlich, G. Erker, *Dalton Trans.* **2008**, 3339–3344; b) I. Saeed, M. Shiotsuki, T. Masuda, *J. Mol. Catal. A* **2006**, *254*, 124–130.

[13] C–F activation reactions at Rh are known but usually more difficult to realize; see, for example: a) M. Kuehnel, D. Lentz, T. Braun, *Angew. Chem. Int. Ed.* **2013**, *52*, 3328–3348; *Angew. Chem.* **2013**, *125*, 2–24; b) T. Braun, F. Wehmeier, *Eur. J. Inorg. Chem.* **2011**, 613–625; c) M. Teltewskoi, J. A. Panetier, S. A. Macgregor, T. Braun, *Angew. Chem. Int. Ed.* **2010**, *49*, 3947–3951; *Angew. Chem.* **2010**, *122*, 4039–4043; d) G. Meier, T. Braun, *Angew. Chem. Int. Ed.* **2009**, *48*, 1546–1548; *Angew. Chem.* **2009**, *121*, 1575–1577.

[14] a) T. Braun, *Organometallics* **2012**, *31*, 1213–1215; b) M. Ahijado, T. Braun, D. Noveski, N. Kocher, B. Neumann, D. Stalke, H.-G. Stammler, *Angew. Chem. Int. Ed.* **2005**, *44*, 6947–6951; *Angew. Chem.* **2005**, *117*, 7107–7111; c) M. Ahijado, T. Braun, *Angew. Chem. Int. Ed.* **2008**, *47*, 2954–2958; *Angew. Chem.* **2008**, *120*, 2996–3000; d) M. Ahijado Salomon, T. Braun, A. Penner, *Angew. Chem. Int. Ed.* **2008**, *47*, 8867–8871; *Angew. Chem.* **2008**, *120*, 8999–9003; e) A.-K. Jungton, P. Kläring, T. Braun, A. Eißler, *Z. Anorg. Allg. Chem.* **2012**, *638*, 505–511; f) P. Kläring, S. Pahl, T. Braun, A. Penner, *Dalton Trans.* **2011**, *40*, 6785–6791; g) M. Ahijado-Salomon, A.-K. Jungton, T. Braun, *Dalton Trans.* **2009**, 7669–7677; h) M. Ahijado-Salo-

mon, T. Braun, I. Krossing, *Dalton Trans.* **2008**, 5197–5206; i) A. Steffen, T. Braun, B. Neumann, H.-G. Stammler, *Angew. Chem. Int. Ed.* **2007**, *46*, 8674–8678; *Angew. Chem.* **2007**, *119*, 8828–8832; j) G. Meier, T. Braun, *Angew. Chem. Int. Ed.* **2011**, *50*, 3280–3284; *Angew. Chem.* **2011**, *123*, 3338–3342; k) G. Meier, T. Braun, *Angew. Chem. Int. Ed.* **2012**, *51*, 12564–12569; *Angew. Chem.* **2012**, *124*, 12732–12737; l) T. Braun, B. Blöcker, V. Schorlemer, B. Neumann, A. Stammler, H.-G. Stammler, *J. Chem. Soc., Dalton Trans.* **2002**, 2213–2218.

[15] A. Panda, M. Stender, R. J. Wright, M. M. Olmstead, P. Klavins, P. P. Power, *Inorg. Chem.* **2002**, *41*, 3909–3916.

[16] a) D. Vidovic, J. A. Moore, J. N. Jones, A. H. Cowley, *J. Am. Chem. Soc.* **2005**, *127*, 4566–4567; b) D. Vidovic, J. N. Jones, J. A. Moore, A. H. Cowley, *Z. Anorg. Allg. Chem.* **2005**, *631*, 2888–2892; c) Z. Yang, H. Zhu, X. Ma, J. Chai, H. W. Roesky, C. He, J. Magull, H.-G. Schmidt, M. Noltemeyer, *Inorg. Chem.* **2006**, *45*, 1823–1827; d) D. Vidovic, Z. Lu, G. Reeske, J. A. Moore, A. H. Cowley, *Chem. Commun.* **2006**, 3501–3503; e) D. Vidovic, M. Findlater, G. Reeske, A. H. Cowley, *J. Organomet. Chem.* **2007**, *692*, 5683–5686; f) D. Vidovic, M. Findlater, A. H. Cowley, *J. Am. Chem. Soc.* **2007**, *129*, 8436–8437; g) G. Xie, C. Qian, *J. Polym. Sci., Part A* **2008**, *46*, 211–217.

[17] a) A. Haaland, *J. Mol. Struct.* **1983**, *97*, 115–128; b) R. Blom, A. Haaland, *J. Mol. Struct.* **1985**, *128*, 21–27.

[18] J. C. Gordon, P. Shukla, A. H. Cowley, J. N. Jones, D. W. Keogh, B. L. Scott, *Chem. Commun.* **2002**, 2710–2711.

[19] a) W.-Y. Lee, H.-H. Hsieh, C.-C. Hsieh, H. M. Lee, G.-H. Lee, J.-H. Huang, T.-C. Wu, S.-H. Chuang, *J. Organomet. Chem.* **2007**, *692*, 1131–1137; b) W.-P. Ye, X.-C. Shi, B.-X. Li, J.-Y. Liu, Y.-S. Li, Y.-X. Cheng, N.-H. Hu, *Dalton Trans.* **2010**, *39*, 9000–9007; c) H. Peng, Z. Zhang, R. Qi, Y. Yao, Y. Zhang, Q. Shen, Y. Cheng, *Inorg. Chem.* **2008**, *47*, 9828–9835; d) H.-K. Shin, M. J. Hampden-Smith, T. T. Kodas, A. L. Rheingold, *J. Chem. Soc., Chem. Commun.* **1992**, 217–219; e) N. H. Cromwell, *Chem. Rev.* **1946**, *38*, 83–137; f) A. Gomtsyan, *Org. Lett.* **2000**, *2*, 11–13; g) D. D. Schnaars, E. R. Batista, A. J. Gaunt, T. W. Hayton, I. May, S. D. Reilly, B. L. Scott, G. Wua, *Chem. Commun.* **2011**, *47*, 7647–7649; h) D. M. Granum, P. J. Riedel, J. A. Crawford, T. K. Mahle, C. M. Wyss, A. K. Begej, N. Arulsamy, B. S. Pierce, M. P. Mehn, *Dalton Trans.* **2011**, *40*, 5881–5890; i) X. He, Y. Yao, X. Luo, J. Zhang, Y. Liu, L. Zhang, Q. Wu, *Organometallics* **2003**, *22*, 4952–4957; j) L. A. Lesikar, A. F. Gushwa, A. F. Richards, *J. Organomet. Chem.* **2008**, *693*, 3245–3255; k) E. Gallo, E. Solari, C. Floriani, A. Chiesi-Villa, C. Rizzoli, *Inorg. Chem.* **1997**, *36*, 2178–2186.

[20] a) Y. S. Varshavsky, E. P. Shestakova, N. V. Kiseleva, T. G. Cherkasova, N. A. Buzina, L. S. Bresler, V. A. Kormer, *J. Organomet. Chem.* **1979**, *170*, 81–93; b) G. S. McNulty, K. Cannon, J. Schwartz, *Inorg. Chem.* **1986**, *25*, 2919–2922; c) N. Dunwoody, S.-S. Sun, A. J. Lees, *Inorg. Chem.* **2000**, *39*, 4442–4451; d) H. E. Fischer, J. Schwartz, *J. Am. Chem. Soc.* **1989**, *111*, 7644–7645; e) S. T. Belt, F. W. Grevels, W. E. Klotzbuecher, A. McCamley, R. N. Perutz, *J. Am. Chem. Soc.* **1989**, *111*, 8373–8382; f) M. Montag, L. Schwartsburd, R. Cohen, G. Leitus, Y. Ben-David, J. M. L. Martin, D. Milstein, *Angew. Chem. Int. Ed.* **2007**, *46*, 1901–1904; *Angew. Chem.* **2007**, *119*, 1933–1936; g) W. I. Dzik, C. Creusen, R. de Gelder, T. P. J. Peters, J. M. M. Smits, B. de Bruin, *Organometallics* **2010**, *29*, 1629–1641.

[21] a) J. A. McCleverty, G. Wilkinson, *Inorg. Synth.* **1990**, *28*, 84–86; b) R. Cramer, *Inorg. Synth.* **1974**, *15*, 14–18; c) F. Malbosc, V. Chauby, C. Serra-Le Berre, M. Etienne, J. Daran, P. Kalck, *Eur. J. Inorg. Chem.* **2001**, 2689–2697.

[22] a) A. Penner, T. Schröder, T. Braun, B. Ziemer, *Eur. J. Inorg. Chem.* **2009**, 4464–4470; b) A. Penner, T. Braun, *Eur. J. Inorg. Chem.* **2011**, 2579–2587; c) A. Eißler, P. Kläring, F. Emmerling, T. Braun, *Eur. J. Inorg. Chem.* **2013**, *27*, 4775–4788.

[23] a) H.-A. Ho, T. S. Gray, B. Baird, A. Ellern, A. D. Sadow, *Dalton Trans.* **2011**, *40*, 6500–6514; b) J. Vicente, J. Gil-Rubio, J. Guerrero-Leal, D. Bautista, *Organometallics* **2004**, *23*, 4871–4881; c) M. P. García, A. P. Martínez, M. V. Jiménez, C. Siurana, L. A. Oro, F. J. Lahoz, A. Tiripicchio, *Inorg. Chim. Acta* **2000**, *308*, 51–58; d) A. J. Esswein, J. L. Dempsey, D. G. Nocera, *Inorg. Chem.* **2007**, *46*, 2362–2364; e) R. Kuwae, T. Tanaka, *Bull. Chem. Soc. Jpn.* **1980**, *53*, 118–120; f) J. C. Jeffrey, V. N. Lebedev, F. G. A. Stone, *Inorg. Chem.* **1996**, *35*, 2967–2976; g) R. Dorta, L. J. W. Shimon, H. Rozenberg, D. Milstein, *Eur. J. Inorg. Chem.* **2002**, *7*, 1827–1834; h) M. Ohashi, A. Shima, T. Rüffer, H. Mizomoto, Y. Kaneda, K. Mashima, *Inorg. Chem.* **2007**, *46*, 6702–6714; i) A. F. Hill, J. D. E. T. Wilton-Ely, *Organometallics* **1997**, *16*, 4517–4518; j) T. O. Northcutt, R. J. Lachicotte, W. D. Jones, *Organometallics* **1998**, *17*, 5148–5152; k) J. A. Kautz, D. A. Kissounko, N. S. Kissounko, F. G. A. Stone, *J. Organomet. Chem.* **2002**, *651*, 34–43; l) M. Sakamoto, Y. Ohki, K. Tatsumi, *Organometallics* **2010**, *29*, 1761–1770; m) L. T.-L. Lo, C.-O. Ng, H. Feng, C.-C. Ko, *Organometallics* **2009**, *28*, 3597–3600; n) L. T.-L. Lo, W.-K. Chu, C.-Y. Tam, S.-M. Yiu, C.-C. Ko, S.-K. Chiu, *Organometallics* **2011**, *30*, 5873–5881; o) C. Tejel, M. A. Ciriano, A. J. Edwards, F. J. Lahoz, L. A. Oro, *Organometallics* **1997**, *16*, 45–53.

[24] a) R. Lindner, B. van den Bosch, M. Lutz, J. N. H. Reek, J. I. van der Vlugt, *Organometallics* **2011**, *30*, 499–510; b) T. S. Teets, T. R. Cook, B. D. McCarthy, D. G. Nocera, *Inorg. Chem.* **2011**, *50*, 5223–5233; c) S. Wanniarachchi, J. S. Hewage, S. V. Lindeman, J. R. Gardinier, *Organometallics* **2013**, *32*, 2885–2888; d) M. Benouazzane, S. Coco, P. Espinet, J. M. Martín-Alvarez, *J. Mater. Chem.* **1999**, *9*, 2327–2332; e) K. Nakamoto, *Infrared Spectra of Inorganic and Coordination Compounds*, John Wiley & Sons, New York **1986**, p. 86–87, and references therein.

[25] a) C. A. James, D. E. Morris, S. K. Doorn, C. A. Arrington Jr., K. R. Dunbar, G. M. Finnis, L. E. Pence, W. H. Woodruff, *Inorg. Chim. Acta* **1996**, *242*, 91–96; b) M. E. Prater, L. E. Pence, R. Clérac, G. M. Finniss, C. Campana, P. Auban-Senzier, D. Jérome, E. Canadell, K. R. Dunbar, *J. Am. Chem. Soc.* **1999**, *121*, 8005–8016; c) S. Martinengo, D. Strumolo, P. Chini, V. G. Albano, D. Braga, *J. Chem. Soc., Dalton Trans.* **1984**, 1837–1841.

[26] Y.-C. Gao, Q.-Z. Shi, D. L. Kershner, F. Basolo, *Inorg. Chem.* **1988**, *27*, 188–191.

[27] a) R. F. Winter, T. Scheiring, *Z. Anorg. Allg. Chem.* **2000**, *626*, 1196–1204; b) T. Murahashi, T. Nagai, T. Okuno, T. Matsutani, H. Kurosawa, *Chem. Commun.* **2000**, 1689–1690; c) M. A. S. Aquino, D. H. Macartney, *Inorg. Chem.* **1987**, *26*, 2696–2699.

[28] a) M. Teltewskoi, S. Kalläne, T. Braun, R. Herrmann, *Eur. J. Inorg. Chem.* **2013**, *33*, 5762–5768 and references cited therein; b) J. I. van der Vlugt, *Chem. Soc. Rev.* **2010**, *39*, 2302–2322; c) J. Zhao, A. S. Goldman, J. F. Hartwig, *Science* **2005**, *307*, 1080–1082; d) A. L. Casalnuovo, J. C. Calabrese, D. Milstein, *Inorg. Chem.* **1987**, *26*, 971–973; e) R. Koelliker, D. Milstein, *Angew. Chem. Int. Ed. Engl.* **1991**, *30*, 707–709; *Angew. Chem.* **1991**, *103*, 724–726; f) T. Braun, *Angew. Chem. Int. Ed.* **2005**, *44*, 5012–5014; *Angew. Chem.* **2005**, *117*, 5138–5140.

[29] A. Vigalok, L. J. W. Shimon, D. Milstein, *Chem. Commun.* **1996**, 1673–1674.

[30] a) G. Balimann, P. S. Pregosin, *J. Magn. Reson.* **1976**, *22*, 235–241; b) T. G. Appleton, M. A. Bennett, *Inorg. Chem.* **1978**, *17*, 738–747; c) A. Castellanos-Páez, S. Castillón, C. Claver, *Organometallics* **1998**, *17*, 2543–2552; d) D. Crozet, D. McKay, C. Bijani, A. Gual, C. Godard, C. Claver, L. Maron, M. Urrutigoïty, P. Kalck, *Dalton Trans.* **2012**, *41*, 3369–3373; e) P. Kläring, A.-K. Jungton, T. Braun, C. Müller, *Eur. J. Inorg. Chem.* **2012**, 1430–1436.

[31] a) B. J. Aylett, M. A. Beckett, *Synth. React. Inorg. Met.-Org. Chem.* **1994**, *24*, 339–344; b) M.-J. Fernandez, P. M. Maitlis, *J. Chem. Soc., Chem. Commun.* **1982**, 310–311; c) R. A. Periana, R. G. Bergman, *J. Am. Chem. Soc.* **1986**, *108*, 7332–7346; d) J. Ruiz, P. O. Bentz, B. E. Mann, C. M. Spencer, B. F. Taylor, P. M. Maitlis, *J. Chem. Soc., Dalton Trans.* **1987**, 2709–2713; e)

S. B. Duckett, D. M. Haddleton, S. A. Jackson, R. N. Perutz, M. Poliakoff, R. K. Upmacis, *Organometallics* **1988**, *7*, 1526–1533; f) T. Braun, D. Noveski, M. Ahijado, F. Wehmeier, *Dalton Trans.* **2007**, 5118–5132; g) T. Braun, F. Wehmeier, K. Altenhöner, *Angew. Chem. Int. Ed.* **2007**, *46*, 5321–5324; *Angew. Chem.* **2007**, *119*, 5415–5418; h) A. L. Raza, J. Panetier, M. Teltewskoi, S. Macgregor, T. Braun, *Organometallics* **2013**, *32*, 3795–3807.

[32] G. R. Fulmer, A. J. M. Miller, N. H. Sherden, H. E. Gottlieb, A. Nudelman, B. M. Stoltz, J. E. Bercaw, K. I. Goldberg, *Organometallics* **2010**, *29*, 2176–2179.

[33] J. Firl, W. Runge, *Angew. Chem. Int. Ed. Engl.* **1973**, *12*, 668–669; *Angew. Chem.* **1973**, *85*, 671–672.

[34] D. E. Webster, *J. Chem. Soc.* **1960**, 5132–5138.

[35] J. L. McBee, J. Escalada, T. D. Tilley, *J. Am. Chem. Soc.* **2009**, *131*, 12703–12713.

[36] a) K. Hübler, P. A. Hunt, S. M. Maddock, C. E. F. Rickard, W. R. Roper, D. M. Salter, P. Schwerdtfeger, L. J. Wright, *Organometallics* **1997**, *16*, 5076–5083; b) A. D. Berry, E. R. Corey, A. P. Hagen, A. G. MacDiarmid, F. E. Saalfeld, B. B. Wayland, *J. Am. Chem. Soc.* **1970**, *92*, 1940–1945; c) X. L. Luo, D. Baudry, P. Boydell, P. Charpin, M. Nierlich, M. Ephritikhine, R. H. Crabtree, *Inorg. Chem.* **1990**, *29*, 1511–1517; d) I. Novak, W. Huang, L. Luo, H. H. Huang, H. G. Ang, C. E. Zybill, *Organometallics* **1997**, *16*, 1567–1572; e) C. J. Levy, R. J. Puddephatt, J. J. Vittal, *Organometallics* **1994**, *13*, 1559–1560; f) C. J. Levy, R. J. Puddephatt, *Organometallics* **1995**, *14*, 5019–5020; g) C. J. Levy, J. J. Vittal, R. J. Puddephatt, *Organometallics* **1996**, *15*, 2108–2117; h) F. S. M. Hassan, S. J. Higgins, G. B. Jacobsen, B. L. Shaw, M. Thornton-Pett, *J. Chem. Soc., Dalton Trans.* **1988**, 3011–3016.

[37] a) L. Zámostná, M. Ahrens, T. Braun, *J. Fluorine Chem.* **2013**, *155*, 132–142; b) L. Zámostná, T. Braun, B. Braun, *Angew. Chem. Int. Ed.* **2014**, *53*, 2745–2749; *Angew. Chem.* **2014**, *126*, 2783–2787.

[38] a) M. H. Mobarok, O. Oke, M. J. Ferguson, R. McDonald, M. Cowie, *Inorg. Chem.* **2010**, *49*, 11556–11572; b) Y. Nishihara, M. Takemura, K. Osakada, *Inorg. Chim. Acta* **2009**, *362*, 2951–2956; c) M. S. Driver, J. F. Hartwig, *Organometallics* **1998**, *17*, 1134–1143; d) A. A. Purwoko, A. J. Lees, *Inorg. Chem.* **1996**, *35*, 675–682; e) M. A. Esteruelas, M. Oliván, L. A. Oro, *Organometallics* **1996**, *15*, 814–822; f) M. Aizenberg, R. Goikhman, D. Milstein, *Organometallics* **1996**, *15*, 1075–1078; g) M. K. Hays, R. Eisenberg, *Inorg. Chem.* **1991**, *30*, 2623–2630; h) C. E. Johnson, R. Eisenberg, *J. Am. Chem. Soc.* **1985**, *107*, 6531–6540.

[39] W. Wolfenberger, H. Schmidtbauer, *Synth. React. Inorg. Met.-Org. Chem.* **1974**, *4*, 149–156.

[40] D. T. Carey, E. K. Cope-Eatough, E. Vilaplana-Mafé, F. S. Mair, R. G. Pritchard, J. E. Warren, R. J. Woods, *Dalton Trans.* **2003**, 1083–1093.

[41] G. Giordano, R. H. Crabtree, *Inorg. Synth.* **1990**, *28*, 88.

[42] R. Cramer, *Inorg. Synth.* **1990**, *28*, 86.

[43] A. van der Ent, A. L. Onderdelinden, *Inorg. Synth.* **1990**, *28*, 90.

[44] a) J. A. McCleverty, G. Wilkinson, *Inorg. Synth.* **1990**, *28*, 84–86; b) R. Cramer, *Inorg. Synth.* **1974**, *15*, 14–18; c) F. Malbosc, V. Chauby, C. Serra-Le Berre, M. Etienne, J. Daran, P. Kalck, *Eur. J. Inorg. Chem.* **2001**, 2689–2697.

[45] M. J. Frisch, G. W. Trucks, H. B. Schlegel, G. E. Scuseria, M. A. Robb, J. R. Cheeseman, G. Scalmani, V. Barone, B. Mennucci, G. A. Petersson, H. Nakatsuji, M. Caricato, H. P. H. X. Li, A. F. Izmaylov, G. Z. J. Bloino, J. L. Sonnenberg, M. Hada, M. Ehara, K. Toyota, R. Fukuda, J. Hasegawa, M. Ishida, T. Nakajima, Y. Honda, O. Kitao, H. Nakai, T. Vreven, J. J. A. Montgomery, J. E. Peralta, F. Ogliaro, M. Bearpark, J. J. Heyd, E. Brothers, K. N. Kudin, V. N. Staroverov, T. Keith, R. Kobayashi, J. Normand, K. Raghavachari, A. Rendell, J. C. Burant, S. S. Iyengar, J. Tomasi, M. Cossi, N. Rega, J. M. Millam, M. Klene, J. E. Knox, J. B. Cross, V. Bakken, C. Adamo, J. Jaramillo, R. Gomperts, R. E. Stratmann, O. Yazyev, A. J. Austin, R. Cammi, C. Pomelli, J. W. Ochterski, R. L. Martin, K. Morokuma, V. G. Zakrzewski, G. A. Voth, P. Salvador, J. J. Dannenberg, S. Dapprich, A. D. Daniels, O. Farkas, J. B. Foresman, J. V. Ortiz, J. Cioslowski, D. J. Fox, *Gaussian 09*, Revision C.01, Gaussian Inc., Wallingford, CT, **2010**.

[46] K. A. Peterson, D. Figgen, H. S. M. Dolg, H. Stoll, *J. Chem. Phys.* **2007**, *126*, 124101–124112.

[47] a) G. M. Shelrick, *SHELXL-2013, Program for Crystal Structure Refinement*, Universität Göttingen, **2013**; b) G. M. Sheldrick, *Acta Crystallogr., Sect. A* **2008**, *64*, 112–122.

[48] A. Altomare, M. C. Burla, M. Camalli, G. L. Cascarano, C. Giacovazzo, A. Guagliardi, A. G. G. Moliterni, G. Polidori, G. Spagna, R. Spagna, *J. Appl. Crystallogr.* **1999**, *32*, 115–119.

Received: February 20, 2014
Published Online: May 16, 2014

